 doi:10.20944/preprints201910.0252.v1

Research Article

Iron depletion Reduces *Abce1* Transcripts While Inducing the Mitophagy Factors *Pink1* and *Parkin*

Jana Key [1,2], Nesli Ece Sen [1], Aleksandar Arsovic [1], Stella Krämer [1], Robert Hülse [1], Suzana Gispert-Sanchez [1] and Georg Auburger [1,*]

[1] Experimental Neurology, Goethe University Medical School, 60590 Frankfurt am Main;
[2] Faculty of Biosciences, Goethe-University Frankfurt am Main, Germany
* Correspondence: auburger@em.uni-frankfurt.de

Abstract: Lifespan extension was recently achieved in *Caenorhabditis elegans* nematodes by mitochondrial stress and mitophagy, triggered via iron depletion. Conversely in man, deficient mitophagy due to *Pink1*/*Parkin* mutations triggers iron accumulation in patient brain and limits survival. We now aimed to identify murine fibroblast factors, which adapt their mRNA expression to acute iron manipulation, relate to mitochondrial dysfunction and may influence survival. After iron depletion, expression of the plasma membrane receptor *Tfrc* with its activator *Ireb2*, the mitochondrial membrane transporter *Abcb10*, the heme-release factor *Pgrmc1*, the heme-degradation enzyme *Hmox1*, the heme-binding cholesterol metabolizer *Cyp46a1*, as well as the mitophagy regulators *Pink1* and *Parkin* showed a negative correlation to iron levels. After iron overload, these factors did not change expression. Conversely, a positive correlation of mRNA levels with both conditions of iron availability was observed for the endosomal factors *Slc11a2* and *Steap2*, as well as for the iron-sulfur-cluster (ISC)-containing factors *Ppat*, *Bdh2* and *Nthl1*. Positive correlation only after iron depletion was observed for the iron export factor *Slc40a1*, mitochondrial iron transporters *Slc25a28*, *Abcb7* and *Abcb8*, mitochondrial ISC-containing factors *Glrx5*, *Nfu1*, *Bola1* and *Abce1*, cytosolic *Aco1* and *Tyw5*, as well as nuclear *Dna2*, *Elp3*, *Pold1* and *Prim2*. The latter are regulators of nucleotide synthesis and DNA quality control, which have known importance for growth and lifespan. The only *Pink1*$^{-/-}$ triggered transcript modulation was the reduced expression of the ISC-containing ribosomal factor *Abce1*. These mammalian findings support previous fly data that Pink1 influences co-translational quality control via *Abce1*, as well as mitophagy. Our findings provide the first systematic survey how iron dosage triggers homeostatic transcriptional regulations and elucidate how iron deprivation results in mitophagy.

Keywords: ferric ammonium citrate, deferoxamine, 2,2′-bipyridine, iron homeostasis, ISC, mitochondrial clearance, longevity, starvation, Parkinson's disease

1. Introduction

Human desire to modify longevity by extrinsic factors such as diet or by modulation of gene activity has triggered intense research. We want to shorten the survival of cancer cells [1] and to prolong lifespan for patients with neurodegenerative disorders [2]. In absence of disease, it is our goal to extend the health period far into old age. Preliminary insights into the underlying mechanisms already exist. Lifespan extension in model organisms was observed for hundreds of gene defects that trigger dietary restrictions via pathways such as insulin signaling, mTOR signaling, and the mitochondrial energy production. Antioxidant defense, stress resistance, maintenance and repair pathways will maintain fitness and extend survival, while cumulative stochastic RNA/DNA damage events will ultimately determine cell death [3-6].

Recently it was shown in *Caenorhabditis elegans* nematodes that an extrinsic factor, namely iron availability, has a strong impact on lifespan. The suppression of iron uptake by a chelator drug, as

 doi:10.20944/preprints201910.0252.v1

well as the silencing of frataxin (Fxn) as a mitochondrial iron-sulfur-cluster (ISC) biogenesis factor, both extended the lifespan via mitochondrial stress and activation of Pink1/Parkin-dependent mitophagy. Downstream effects of this pathological scenario included the elevated expression of globins, which bind to iron in the form of heme [7]. It was also reported that natural inducers of mitophagy, such as urolithin A, can extend lifespan in *C. elegans* [8]. We were intrigued by these observations, since a converse situation is observed in man: Defective mitophagy due to *Pink1*/*Parkin* mutations shortens the lifespan and leads to the accumulation of iron, in a process that we know as Parkinson's disease (PD) [9-11].

The serine-threonine kinase Pink1 is associated with the outer mitochondrial membrane and plays a major role in the Pink1-Parkin dependent autophagic degradation of damaged or aged mitochondria, a process known as mitophagy [12-14]. *Pink1* and *Parkin* get transcriptionally induced in human neuroblastoma cells after serum deprivation or nutrient starvation [15], linking nutrient restriction to mitophagy. Mutations in *Pink1* lead to an autosomal recessive form of PD, which was named PARK6 [10, 16]. Iron distribution is altered in brains of all PD patients [17, 18], with an increase of iron levels in the midbrain substantia nigra [19, 20], where loss of dopaminergic neurons is observed. These findings add to the established theory that iron accumulation contributes to neurodegenerative processes. It remains unclear whether pathological redistribution of the excess iron to ferritin, the labile iron pool and mitochondria occurs, or if altered turnover of iron-containing proteins is responsible for the iron toxicity in PD. One piece of evidence was found in a neurotoxic PD model via 5-day acute exposure to the respiratory complex-I inhibitor MPTP (1-methyl-4-phenyl-1,2,3,6-tetrahydropyridine), where an increase of ferritin light-chain and mitoferritin was documented together with a protective function of mitoferritin overexpression [21].

Detailed studies of PD pathogenesis confirmed that (i) *Pink1* mutations trigger iron accumulation in the midbrain of patients [22], (ii) *Pink1* deficiency-mediated iron accumulation may involve degradation of mitochondrial membrane iron transporters Slc25a37 and Slc25a28 [23, 24], (iii) iron chelation-induced mitophagy can be observed in patient primary fibroblasts [25], (iv) *Pink1*-dependent phenotypes in flies can be suppressed by mitochondrial aconitase (Aco2), while superoxide-dependent inactivation of the Aco2 [4Fe-4S] cluster triggers iron toxicity that is reversed by mitoferritin overexpression [26]. Thus, there is a close link between the mitochondrial dysfunction underlying PD on the one hand, with the homeostasis of iron, ISC, and heme on the other hand. It is important now to elucidate the relevant molecular events, to define biomarkers of PD progression and to understand how extrinsic factors may modify the disease course.

In the chronic state of mutant brain tissue, it is very hard to detect these anomalies. Mitophagy is relevant for only a few among hundreds or thousands of mitochondria per cell at any given time, and the accumulation of iron is an insidious process over decades in PD patients, so the compensatory efforts needed are minimal. Therefore, global expression profiles of *Pink1*$^{-/-}$ mouse brain showed only subtle evidence of deficient mitophagy and altered mitochondrial biogenesis [16, 27-29], the dysregulated expression of heme-related transcripts *Hmox1* and *Hebp1* was noted only upon culture of mouse *Pink1*$^{-/-}$ primary cortical neurons [29], and limited survival of the *Pink1*$^{-/-}$ mouse was observed only after additional overexpression of toxic alpha-synuclein [16, 30]. In general, Pink1- and Parkin-deficient mice show signs of altered mitophagy and neurodegeneration only in the presence of further stressors such as mitochondrial mutations, exhaustive exercise or bacterial infections [31-34]. Also in *C. elegans Pink1*- and *Parkin*-mutants, a lifespan effect was undetectable. In contrast, the survival of *Drosophila melanogaster* flies with depletion of *Pink1* or of *Parkin* was significantly shortened by a degeneration of wing muscles, due to the massive exercise and energetic demand during flight [16, 35-37].

Not only altered mitophagy, but autophagy and mitochondrial dysfunction in general have strong effects on iron homeostasis and lifespan, as was demonstrated in *C. elegans* for the so-called mit-mutants [38-40]. In a well-established model of rapid ageing, the fungus *Podospora anserina*, a simple depletion of the mitochondrial matrix protease ClpP results in prolonged lifespan [41]. Again, mice with *ClpP* deletion were shown to have altered survival with higher resistance to metabolic stress and bacterial infections [42, 43], as well as iron and hemoglobin accumulation

 doi:10.20944/preprints201910.0252.v1

(https://www.mousephenotype.org/data/genes/MGI:1858213). In contrast to *Pink1* mutant cells [13, 44], stable *ClpP* mutants showed no evidence of oxidative stress [45], enhancing the doubts whether reactive oxygen species (ROS) have a central process in the control of lifespan [46, 47].

Intracellular iron metabolism in mammalian cells is crucial for their proper functions. Free iron molecules can be toxic to cells, leading to the production of ROS, so there have to be strict regulatory mechanisms. Iron metabolism affects the whole cell, since iron is taken up from extracellular space either via transferrin or in a transferrin-independent manner, then reduced in lysosomes for detoxification and distributed within cells, for example to mitochondria, where iron is utilized for ISC production and heme generation [48-50]. The correct function of dozens of proteins in mitochondria, cytosol and nucleus depends on the insertion of ISC [51, 52], so the regulation of iron homeostasis is crucial. ISC play important roles in a wide range of cellular reactions, e.g. electron transfer, catalysis of enzymatic reactions, regulation of gene expression and the quality control of nucleotides, thus controlling genome integrity [53-55]. Similarly, heme is needed as cofactor of cytochrome proteins within mitochondria, but also of cytosolic cytochrome P450 proteins, globins, iron-regulatory proteins, peroxidases, catalase and specific ion-channels [56].

For a further elucidation of homeostatic cellular efforts upon acute changes of iron levels, we now exposed murine embryonal fibroblasts (MEF) to iron overload and iron depletion and quantified the transcriptional expression adaptation of crucial factors by reverse transcriptase real-time quantitative polymerase chain reaction (RT-qPCR). Most of these factors have been mutated previously to establish their impact on iron, ISC and heme turnover, but their cellular regulation on-demand was never investigated. We also studied *Pink1* expression and *Pink1*-deleted cells, to understand the regulation of mitophagy and the consequences of altered mitophagy for iron processing. Overall, the data confirm that *Pink1*-dependent mitophagy changes have direct impact on the quality control during ribosomal translation, and that iron is required for sufficient synthesis of surveillance factors for the transcriptome and the genome. Although our studies *in vitro* focused on strong transcription changes of peripheral cells in response to massive acute iron stress and thus are limited to extreme situations never observed *in vivo*, we believe that similar more insidious processes occur in the nervous system and might contribute to neurodegenerative diseases.

2. Results

We wanted to understand (1) how iron manipulation leads to transcriptional adaptations of iron homeostasis factors and iron-associated factors in different cell compartments, and (2) to what degree deficient mitophagy due to *Pink1* deletion generates feedback onto iron homeostasis. MEF cells were exposed to ferric ammonium citrate (FAC) to enhance iron availability. In order to deplete iron from the cell culture medium, we employed two different iron chelators, deferoxamine (DFO) and 2,2'-Bipyridine (22BP). Transcriptional changes after 16 hours were quantified for all three conditions.

2.1 Transcriptional analyses of cellular iron homeostasis factors in wildtype MEF in response to altered iron levels

In the discovery phase of this project, we wanted to account for biological variability and screened a large number of wildtype (WT) MEF for iron-dependent expression regulations. As proof-of-principle for the iron-responsiveness of fibroblast expression profiles, Figure 1A shows the transcriptional response of the transferrin receptor (*Tfrc*), which is the main receptor to import iron into the cell, as well as the iron storage protein ferritin with its heavy chain (Fth1) and light chain (Ftl1). *Tfrc* was reduced only by 0.45-fold under iron excess conditions ($p=0.77$), suggesting that iron levels in the basal culture medium is already so high that transferrin-receptor expression cannot be downregulated much during FAC administration. *Tfrc* was highly induced after DFO (4.66-fold with $p=0.0010$) and after 22BP (3.72-fold with $p=0.0068$). Thus, the main regulator of iron uptake responded

 doi:10.20944/preprints201910.0252.v1

to iron depletion in a sensitive manner. *Fth1* and *Ftl1* were not changed significantly and displayed high variability among the 6 different MEF cell lines, but both ferritin subunit transcripts showed about 2-fold higher levels during iron excess. Conversely, *Slc40a1* mRNA encoding ferroportin-1 as cellular iron exporter showed below 0.5-fold levels during iron depletion (DFO 0.24-fold with p=0.0023, 22BP 0.41-fold with p=0.0107) (Figure 1A). These experiments confirmed that MEF are responsive to manipulation of iron availability, so we performed further studies into their adaptations of mRNA expression, focusing on several factors of the cellular iron transport and mitochondrial homeostasis, of the heme synthesis pathway and hemeproteins, of the ISC biogenesis pathway and of ISC-containing factors.

There were various factors related to these pathways, which showed no significant dysregulations under any condition, or were less relevant or redundant, so they were shown only in the Supplementary Figure S1. In alphabetical order, these factors include *Abcb6*, *Aco1*, *Aco2*, *Alas1*, *Bach1*, *Brip1*, *Cdc42bpa*, *Cisd2*, *Cp*, *Cygb*, *Dpyd*, *Elp3*, *Ercc2*, *Fech*, *Fdx1*, *Flvcr1*, *Fxn*, *Hebp1*, *Ncoa4*, *Pcbp1*, *Pcbp2*, *Prim2*, *Rsad1*, *Rsad2*, *Rtel1*, *Slc25a37*, *Steap3* and *Trf*. The other factors with important dysregulation are shown in the main figures and are individually mentioned in the text below, together with their respective roles.

Preprints (www.preprints.org) | NOT PEER-REVIEWED | Posted: 22 October 2019 doi:10.20944/preprints201910.0252.v1

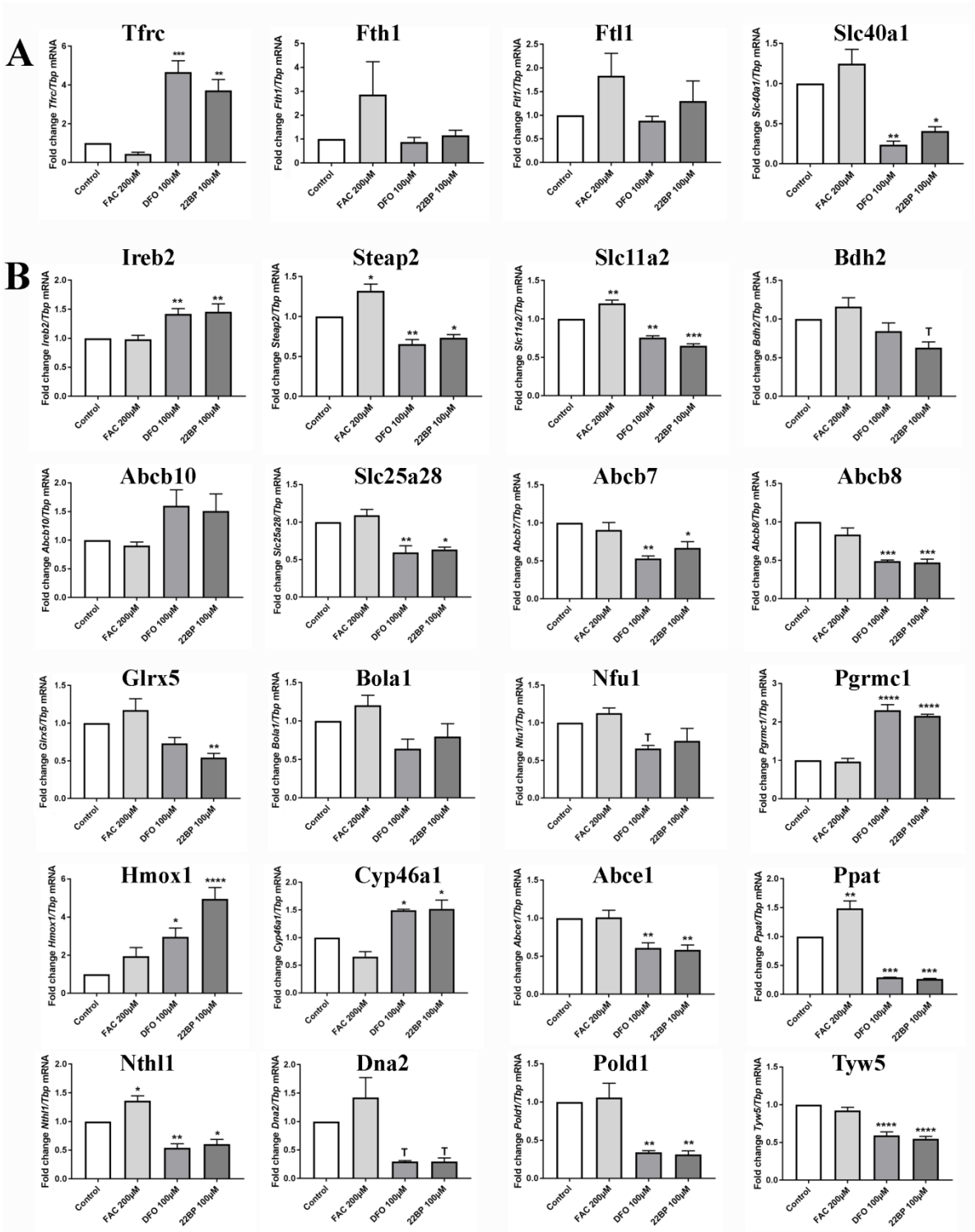

Figure 1. mRNA expression analysis by RT-qPCR in WT MEF (n=6 on average), regarding factors related to **A)** cellular iron uptake and storage, **B)** iron transport and processing, mitochondrial iron homeostasis, heme production / turnover / binding, ISC-biogenesis and ISC-binding. All factors studied are presented in their approximate order of action during cellular iron homeostasis. Their expression adaptation was documented 16 h after iron overload (FAC) or after two different iron depletion conditions (DFO, 22BP). Mean values with SEM are shown, normalized to the control condition. The levels of significance are illustrated by symbols T: 0.1>p>0.05, *: p< 0.05, **: p < 0.01, ***: p < 0.001, ****: p < 0.0001.

Tfrc mRNA is stabilized by Ireb2, whose mRNA was also induced after iron deprivation (Figure 1B). After transferrin binding to Tfrc and subsequent endocytosis of this complex, the acidic pH in

 doi:10.20944/preprints201910.0252.v1

endosomes releases ferric iron (Fe^{3+}), which is reduced to the ferrous form (Fe^{2+}) by the metalloreductases Steap2 and Steap3. Iron molecules then get exported by the divalent metal transporter 1 (DMT1 encoded by *Slc11a2*) to the cytosol. After iron overload, *Steap2* and *Slc11a2* mRNA showed a significant approximately 1.3-fold upregulation (Figure 1B and Suppl. Figure S1), indicating higher biosynthesis of the factors responsible for reduction and export of iron. During both forms of iron depletion, *Steap2* and *Slc11a2* mRNAs were significantly reduced to 0.65-fold, so their levels are in direct correlation with iron availability.

The ISC-containing 3-hydroxybutyrate dehydrogenase-2 (Bdh2) catalyzes the rate-limiting step in the biosynthesis of siderophores, which are soluble Fe^{3+} binding agents. Upon iron depletion, *Bdh2* transcription was slightly downregulated (DFO: 0.84-fold with p=0.5980; 22BP: 0.63-fold with p=0.0655). Bdh2 inhibition was shown to result in cellular iron accumulation [57], so again its expression adaptation could represent a homeostatic effort to increase intracellular iron levels.

The poly(RC) binding protein 2 (Pcbp2) is involved in mRNA metabolism and translation, as well as innate immune signaling, but was previously shown to function also as chaperone for the labile iron pool (LIP) in the cytosol [58]. However, neither *Pcbp2* nor *Pcbp1* transcript were consistently changed by iron level manipulation (Suppl. Figure S1).

The iron regulatory proteins (Irp1 encoded by the *Aco1* mRNA, and Irp2 by *Ireb2*) sense cytosolic iron availability and ensure adequate iron supply to mitochondria [59], firstly via association with iron response elements (IREs) in the untranslated region (UTR) of ferritin mRNA to inhibit its translation, and secondly via association with *Tfrc* mRNA to stabilize it and thus facilitate iron import when cellular iron levels are low. During both forms of iron depletion, the transcription of *Ireb2* showed an upregulation (DFO: 1.42-fold with p=0.0095; 22BP: 1.46-fold with p=0.0042), while *Aco1* showed a consistent reduction (DFO: 0.61-fold with p=0.2894; 22BP: 0.53-fold with p=0.1362; Suppl. Figure S1). Under conditions of sufficient iron, Irp1 exerts its cytosolic aconitase functions while Irp2 gets degraded, resulting in converse effects with increased ferritin translation and Tfrc degradation [60]. After iron overload, we detected no relevant expression adaptation of both transcripts encoding iron regulatory proteins.

Expression of the mitochondrial inner membrane transporter *Slc25a28*, which encodes Mitoferrin 2 (Mfrn2), did not react after iron overload, but was significantly reduced after iron depletion (DFO: 0.60-fold with p=0.0066; 22BP: 0.64-fold with p=0.0119). Mitoferrin 1 (*Slc25a37*), however, did not show consistent alteration upon different iron levels. Mfrn1 forms a complex with the mitochondrial inner membrane iron transporter Abcb10 [61]. *Abcb10* transcript levels were 1.5-fold higher under both iron depletion conditions, but these changes were statistically not significant. Given that it is not clear how these two inner membrane transporters of iron are acting in complementary fashion, it is interesting to note that *Abcb10* mRNA was higher during low iron conditions as expected for an iron uptake factor. However, *Slc25a28* mRNA was diminished under the same treatment, a response that would be in line with an iron export factor. In comparison, *Abcb7* and *Abcb8* are thought to have mitochondrial export functions [62-65] and are also important for heme biosynthesis [66]. As expected after iron depletion, *Abcb7* transcript was reduced (DFO: 0.53-fold with p=0.0042; 22BP: 0.67-fold with p=0.0299), similar to the reduction of *Abcb8* transcript (DFO: 0.49-fold with p=0.0003; 22BP: 0.47-fold with p=0.0003).

Once transported into the mitochondrial matrix, iron may be stored or used for the biosynthesis of ISC and heme. The mitochondrial iron storage factor Mitoferritin (*Ftmt*) was not detectable in MEF cells under the conditions tested. For biosynthesis purposes, iron is incorporated by Fxn into the sulfur-containing Nfs1-Iscu-Lyrm4-complex to generate [2Fe-2S] clusters, which associate with Glrx5 (glutaredoxin 5) and the assembly factor Bola1 (BolA Family Member 1) [49, 67, 68]. Subsequently, these ISC are transferred by the ISC scaffold Nfu1 to target proteins [69]. After both iron depletion conditions, *Glrx5* expression was reduced (DFO: 0.73-fold with p=0.1804; 22BP: 0.54-fold with p=0.0089). *Fxn*, *Bola1* and *Nfu1* levels were around 0.7-fold after both iron depletion conditions (Figure 1B and Suppl. Figure S1), but this was not statistically significant. The converse iron overload did not modulate expression of the ISC biogenesis proteins.

 doi:10.20944/preprints201910.0252.v1

Pursuing the heme- and ISC-associated pathways into the cytosol, it is relevant that the putative heme release factor *Pgrmc1*, as cytosolic factor in association with mitochondrial ferrochelatase, showed a more than two-fold transcriptional induction after iron depletion (DFO: 2.30-fold with p<0.0001; 22BP: 2.16-fold with p<0.0001). Heme oxygenase 1 (Hmox1) acts to degrade cytoplasmic heme by cleaving it to biliverdin, as the rate limiting step of heme breakdown [70]. After iron depletion, *Hmox1* mRNA was highly upregulated (DFO: 2.96-fold with p=0.0249; 22BP: 4.95-fold with p<0.0001). This upregulation might reflect a compensatory cellular effort to recruit iron via heme breakdown. The cholesterol elimination factor Cyp46a1 belongs to the Cytochrome P450 family, which is known to bind heme as a co-factor [71, 72]. After iron depletion, *Cyp46a1* transcript was slightly, but consistently increased (DFO: 1.49-fold with p=0.0232; 22BP: 1.52-fold with p=0.0179); it was not altered after iron overload. Continuing the heme-related pathway, the transcript levels of Cytoglobin (*Cygb*) [73] were quantified, as one vertebrate globin family that is expressed in fibroblasts, but they showed no change and high variability (Suppl. Figure S1).

Not only heme, but also ISC are incorporated into target proteins, many of which have nucleotide processing functions. Among the ISC-containing factors present inside and outside of mitochondria, the essential ribosome recycling factor Abce1 (ATP Binding Cassette Subfamily E Member 1) exerts crucial functions to avoid accumulation of ribosomes at the stop codon, inefficient ribosomal cycling and stalled translation [74, 75]. Interestingly, after both forms of iron depletion a significant decrease of *Abce1* mRNA (DFO: 0.61-fold with p=0.0024; 22BP: 0.58-fold with p=0.0013) was observed, while iron overload triggered no expression adaptation.

The ISC-containing phosphoribosyl pyrophosphate amidotransferase (Ppat=Gpat) is the rate-limiting enzyme in *de novo* purine nucleotide biosynthetic pathways. Its expression showed a strong direct correlation of high significance with the availability of iron. After incubation with FAC, *Ppat* was significantly upregulated (1.49-fold; p=0.0034). After iron depletion it was massively downregulated (DFO: 0.29-fold with p=0.0003; 22BP: 0.27-fold with p=0.0002). These sensitive adaptations suggest that iron has supreme importance for nucleotide homeostasis.

The Nth like DNA glycosylase 1 (Nthl1) has important functions in base excision repair, harbors an ISC and is localized both in the nucleus and the mitochondrial matrix. The expression of *Nthl1* reacted similar to *Ppat* with upregulation after iron overload (1.36-fold; p=0.0274) and downregulation after both forms of iron depletion (DFO: 0.54-fold with p=0.0071; 22BP: 0.61-fold with p=0.0172), although with less effect size and less significance.

Similarly, three other ISC-associated nuclear factors implicated in DNA quality control also showed consistent downregulations after iron deprivation, namely the DNA replication helicase *Dna2* (DFO: 0.30-fold with p=0.0893; 22BP: 0.30-fold with p=0.0897), the DNA primase subunit *Prim2* (DFO: 0.82-fold with p=0.1627; 22BP: 0.84-fold with p=0.2372; Suppl. Figure S1), and the DNA polymerase delta subunit *Pold1* (DFO: 0.34-fold with p=0.0061; 22BP: 0.31-fold with p=0.0042).

The tRNA wybutosine synthesizing protein 5 (Tyw5) was reported to catalyze a carbon hydroxylation using Fe^{2+} ions as cofactors, so its activity depends on iron levels. *Tyw5* expression did not react to iron overload, but it was downregulated with extreme significance after iron depletion (DFO: 0.59-fold with p<0.0001; 22BP: 0.55-fold with p<0.0001).

Jointly, these results in WT cells indicate that upon iron overload and even more upon iron depletion, expression adapts up to two-fold within 16 hours for specific factors at the plasma membrane, in endosomes and the cytosol, inside mitochondria as well as the nucleus. An indirect negative correlation was found for iron transport components at the plasma membrane and mitochondrial membrane, which responded to iron depletion with induced expression of *Tfrc* / *Ireb2* and *Abcb10*, respectively. Similarly, the iron recruitment option via mitochondrial heme release and its cytosolic breakdown responded to iron depletion with induced expression of *Pgrmc1* / *Hmox1*. Furthermore, increased need for the heme-binding cholesterol catabolism enzyme *Cyp46a1* became apparent during iron depletion. In contrast, a strong direct correlation with iron levels was observed for endosomal and cytosolic iron processing factors *Steap2* and *Slc11a2*, exhibiting increased expression upon iron overload versus decreased expression upon iron depletion. A similarly strong direct correlation was also documented for ISC-containing factors of nucleotide metabolism, namely

Preprints (www.preprints.org) | NOT PEER-REVIEWED | Posted: 22 October 2019 doi:10.20944/preprints201910.0252.v1

Ppat and *Nthl1*. All other expression adaptations observed simply reflected the diminished synthesis of iron-associated factors under conditions of low iron levels.

2.2 Transcriptional analyses of cellular iron homeostasis factors in Pink1$^{-/-}$ MEF in response to altered iron levels

In the validation phase of this project, experiments were performed in additional wildtype MEFs and also in *Pink1*-deficient MEFs where mitophagy is impaired. Again, we studied FAC-mediated iron overload and DFO/22BP-mediated iron depletion, now in 3 WT MEF lines versus 3 *Pink1*$^{-/-}$ MEF lines. With this approach we hoped to elucidate how iron, ISC and heme homeostasis relate to mitophagy.

Figure 2A shows mRNA levels of *Pink1* and *Park2* (*Parkin*) as regulators of mitophagy. The first panel confirms the knockout of *Pink1* in the MEF and demonstrates a high transcriptional induction of *Pink1* after iron deficiency (for DFO 1.42-fold with p=0.0006 in WT and 0.30-fold with p=0.0794 in *Pink1*$^{-/-}$ MEF; for 22BP 1.65-fold with p<0.0001 in WT and 0.40-fold with p=0.0076 in *Pink1*$^{-/-}$ MEF). This transcript induction was obviously much less strong in the *Pink1*$^{-/-}$ cells. These *Pink1*$^{-/-}$ MEF derive from a mouse where an intron is retained in the *Pink1*$^{-/-}$ mRNA and triggers a changed reading frame, so *Pink1* mRNA is rapidly degraded and the Pink1 protein is absent, but the *Pink1* promoter is still actively responding to specific stressors like iron depletion. Similarly, the *Park2* transcript got induced upon iron depletion (for 22BP 2.40-fold with p=0.0007 in WT and 1.85-fold with p=0.0065 in *Pink1*$^{-/-}$ MEF). These results in Figure 2A corroborate the concept that Pink1/Parkin-dependent mitophagy gets highly induced after iron starvation in MEF.

Figure 2B shows the transcriptional changes of the key cellular iron turnover factors. Initial cellular iron uptake (*Tfrc*), storage (*Fth1*, *Ftl1*) and cell export (*Slc40a1*) showed no differences between *Pink1*-deficiency and WT, with the transferrin receptor being highly upregulated also in *Pink1*$^{-/-}$ MEF (DFO: 4.66-fold with p<0.0001; 22BP: 3.72-fold with p=0.0009) in response to iron depletion. Upon comparison of Figure 1 with Figure 2B/C, fewer expression adaptations reached statistical significance, due the smaller number of cell lines studied and limited statistical power.

The overall pattern of regulations was reproduced in this second analysis also in Figure 2C and Suppl. Figure S1. Again, a negative correlation was found between iron availability and activators of membrane import, with induced expression after iron depletion for *Tfrc* together with *Ireb2* (for DFO 1.47-fold with p=0.0052 in WT and 1.39-fold with p=0.0244 in *Pink1*$^{-/-}$ cells; for 22BP 1.53-fold with p=0.0020 in WT and 1.32-fold with p=0.0734 in *Pink1*$^{-/-}$ cells) and for the mitochondrial transporter *Abcb10* (DFO: 1.30-fold with p=0.0459 in *Pink1*$^{-/-}$ cells). Similarly, the iron recruitment via mitochondrial heme release as well as heme breakdown reacted to iron depletion with induced expression of *Pgrmc1* (DFO: 2.11-fold with p<0.0001; 22BP: 2.07-fold with p<0.0001 in *Pink1*$^{-/-}$ cells) and of *Hmox1* (22BP: 5.10-fold with p=0.0063 in WT cells), respectively. Again, iron depletion resulted in increased *Cyp46a1* transcript levels (DFO: 1.43-fold with p=0.0259; 22BP: 1.43-fold with p=0.0274), reflecting heme-regulated adaptations.

Conversely again, a positive correlation was observed for endosomal and cytosolic iron processing factors *Steap2* (after FAC 1.32-fold with p=0.0043 in *Pink1*$^{-/-}$ cells), *Slc11a2* (after FAC 1.73-fold with p=0.0393 in *Pink1*$^{-/-}$ cells) and now also for the iron chaperone *Bdh2* (after FAC 1.14-fold with p=0.0323 in *Pink1*$^{-/-}$ MEF; for DFO 0.75-fold with p=0.0622 in WT and 0.69-fold with p=0.3398 in *Pink1*$^{-/-}$ cells; for 22BP 0.65-fold with p=0.0059 in WT and 0.57-fold with p=0.0211 in *Pink1*$^{-/-}$ cells), exhibiting increased expression upon iron overload. The strong positive correlation was also confirmed for ISC-containing factors of nucleotide metabolism, which exhibited increased expression upon iron overload versus decreased expression upon iron depletion. Indeed, *Ppat* was upregulated after iron overload (1.49-fold with p=0.0001 in WT and 1.30-fold with p=0.0137 in *Pink1*$^{-/-}$ MEF), but downregulated after iron depletion (for DFO 0.29-fold with p<0.0001 in WT and 0.31-fold with p<0.0001 in *Pink1*$^{-/-}$ MEF; for 22BP 0.27-fold with p<0.0001 in WT and 0.24-fold with p<0.0001 in *Pink1*$^{-/-}$ MEF). *Nthl1* also was upregulated after iron overload (1.36-fold with p=0.0066 in WT and 1.37-fold with p=0.0003 in *Pink1*$^{-/-}$ MEF), but downregulated after iron depletion (for DFO 0.54-fold with

 doi:10.20944/preprints201910.0252.v1

p=0.0008 in WT and 0.60-fold with p=0.2269 in *Pink1*$^{-/-}$ MEF; for 22BP 0.61-fold with p=0.0032 in WT, 0.43-fold with p=0.0112 in *Pink1*$^{-/-}$ MEF).

The impact of the lack of iron on ISC-containing factors implicated in nucleotide processing was also obvious for the DNA quality control factors *Dna2*, *Prim2* and *Pold1*, as well as the tRNA modifying factor *Tyw5*. They did not show changes after iron overload, but were downregulated strongly after iron depletion (*Dna2* for DFO 0.30-fold with p=0.0208 in WT and 0.33-fold with p=0.0071 in *Pink1*$^{-/-}$ cells; for 22BP 0.30-fold with p=0.0209 in WT and 0.31-fold with p=0.0061 in *Pink1*$^{-/-}$ MEF), (*Prim2* for DFO 0.78-fold with p=0.0189 in *Pink1*$^{-/-}$ cells; for 22BP 0.69-fold with p=0.0026 in *Pink1*$^{-/-}$ MEF, Suppl. Figure S1), (*Pold1* for DFO 0.34-fold with p=0.0002 in WT and 0.27-fold with p=0.0001 in *Pink1*$^{-/-}$ cells; for 22BP 0.31-fold with p=0.0001 in WT and 0.22-fold with p<0.0001 in *Pink1*$^{-/-}$ MEF), (*Tyw5* for DFO 0.50-fold with p<0.0001 in WT and 0.49-fold with p<0.0001 in *Pink1*$^{-/-}$ cells; for 22BP 0.51-fold with p<0.0001 in WT and 0.50-fold with p<0.0001 in *Pink1*$^{-/-}$ MEF).

In *Pink1*$^{-/-}$ MEF, similar responses to iron depletion was also observed in the ISC biogenesis factors *Bola1* (DFO: 0.61-fold with p=0.0201; 22BP: 0.54-fold with p=0.0092) and *Nfu1* (DFO: 0.55-fold with p=0.0100; 22BP: 0.67-fold with p=0.0389), whereas *Glrx5* did not change in the mutant MEF. In addition, the ISC-containing Elongator complex protein 3 (Elp3), which is involved in tRNA modification [76], showed 0.7-fold lower transcript levels after iron depletion (for DFO: 0.75-fold with p=0.0002 in WT and 0.65-fold with p<0.0001 in *Pink1*$^{-/-}$ cells, for 22BP: 0.69-fold with p<0.0001 in WT and 0.68-fold with p=0.0003 in *Pink1*$^{-/-}$ cells) (Suppl. Figure S1).

For the putative iron exporters Abcb7 and Abcb8, the previously observed transcript decreases were also seen in *Pink1*$^{-/-}$ cells, especially in *Abcb8* (0.43-fold with p<0.0001 for DFO and 0.39-fold with p<0.0001 for 22BP).

Interestingly, the downregulation of the mitochondrial membrane transporter *Slc25a28* (encoding Mitoferrin-2) after iron depletion was reproduced in the *Pink1*$^{-/-}$ lines (DFO: 0.63-fold with p=0.0162; 22BP: 0.61-fold with p=0.0108) in agreement with a hypothetical iron export role, while *Slc25a37* (encoding Mitoferrin-1) showed a significant induction after FAC treatment (1.61-fold with p=0.0129 in *Pink1*$^{-/-}$ MEF) as expected for an iron import factor (Suppl. Figure S1).

For several factors, *Pink1*$^{-/-}$ MEF showed significant changes or trends when WT cells did not. This was the case for *Ftl1* after FAC (2.35-fold with p=0.0573), *Slc11a2* after FAC (1.73-fold with p=0.0393), *Slc25a37* after FAC (1.61-fold with p=0.0129) and *Hmox1* after FAC (4.03-fold with p=0.0735), for *Slc40a1* after DFO (0.25-fold with p=0.0729), *Pcbp2* after FAC (0.80-fold with p=0.0804) and DFO (0.75-fold with p=0.0367), *Aco1* after 22BP (0.48-fold with p=0.0277, Suppl. Figure S1), *Bola1* after DFO (0.61-fold with p=0.0201) and 22BP (0.54-fold with p=0.0092), *Abcb10* after DFO (1.30-fold with p=0.0459). Rather than reflecting vulnerability against a specific insult, this may reflect a general role of Pink1 in stress responses, or may simply be due to multiple testing.

The only putative genotype-dependent effect was observed for the ISC-containing ribosome recycling factor and RNase L inhibitor *Abce1*, which revealed slightly lower levels in *Pink1*-deficient cells already under control conditions (0.70-fold with p=0.0571). Interestingly, this was no longer observed after iron overload and during iron depletion, where it was similarly downregulated as in WT control cells.

Preprints (www.preprints.org) | NOT PEER-REVIEWED | Posted: 22 October 2019 doi:10.20944/preprints201910.0252.v1

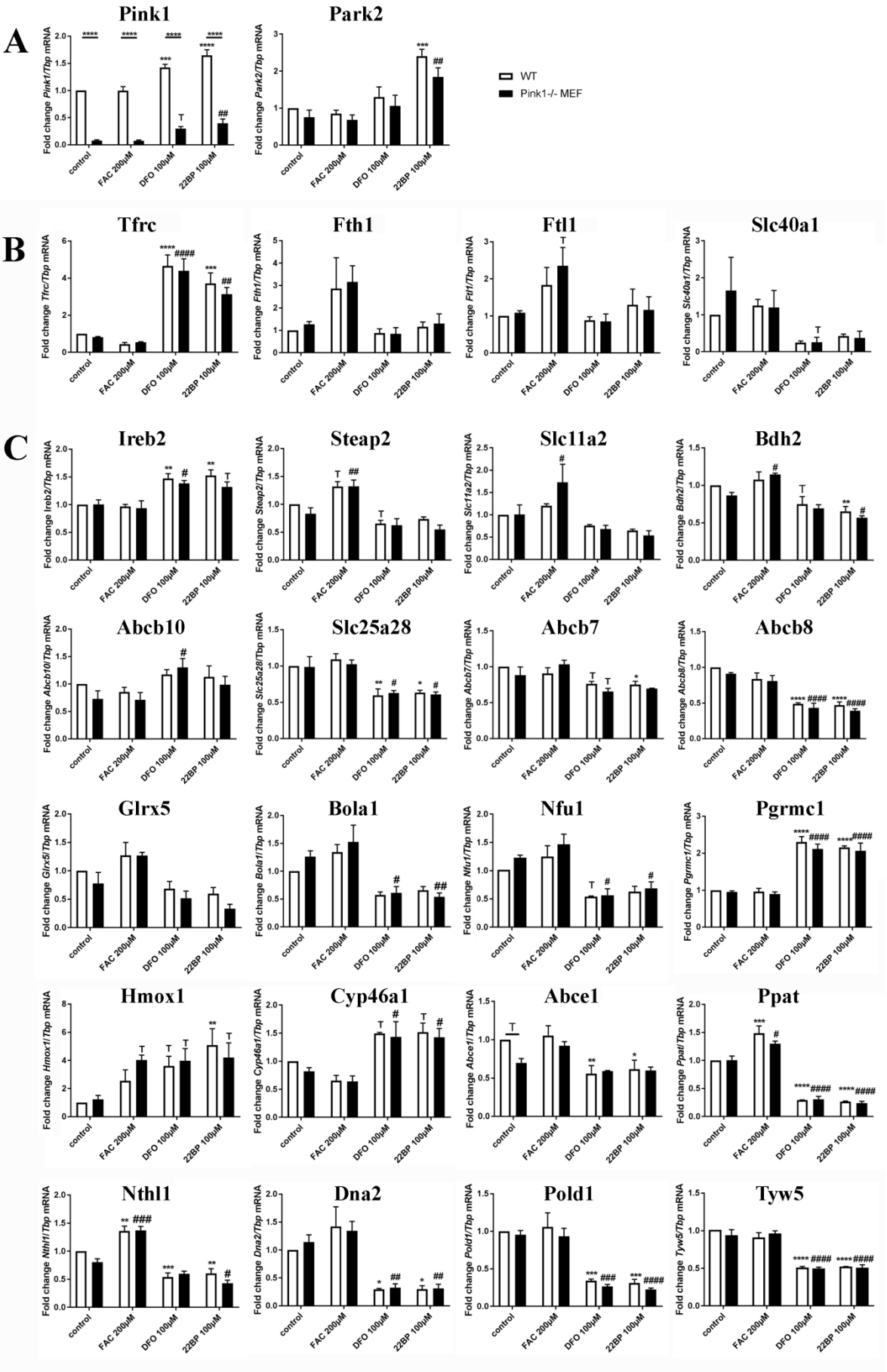

369
370

Preprints (www.preprints.org) | NOT PEER-REVIEWED | Posted: 22 October 2019 doi:10.20944/preprints201910.0252.v1

Figure 2. mRNA expression analysis by RT-qPCR in WT and *Pink1*$^{-/-}$ MEF (n=3versus3) regarding factors related to **A)** the mitophagy modulators *Pink1* and *Park2* after iron manipulation, **B)** cellular iron uptake, storage and export, **C)** iron transport and processing, mitochondrial iron homeostasis, heme production and turnover, ISC-biogenesis and ISC-binding. All factors studied are presented in their approximate order of action during cellular iron homeostasis. Their expression adaptation was documented after iron overload (FAC) and under two different iron depletion conditions (DFO, 22BP). Mean values with SEM are shown, normalized to the control condition. The levels of significance are illustrated by symbols T: 0.1>p>0.05, *: p< 0.05, **: p < 0.01, ***: p < 0.001, ****: p < 0.0001. Asterisks represent significance in wildtype MEF in respect to WT control and hashtags in *Pink1*$^{-/-}$ MEF, in respect to knockout control.

2.3 Analyses of protein levels of PPAT and NFU1 as ISC-containing factors in response to altered iron levels

Now we wanted to assess in further validation experiments if the observed changes can also be seen on protein levels, focusing on three dysregulated factors whose transcript dysregulation had marked effect size and where a promising antibody was available. PPAT contains an ISC and its mRNA had exhibited strong positive correlations with iron levels, with three-fold downregulation after iron depletion; NFU1 is involved in the biosynthesis of ISC and its transcript had shown almost two-fold downregulation after iron depletion; TFRC had shown more than four-fold upregulation after iron deprivation (Figures 1 and 2).

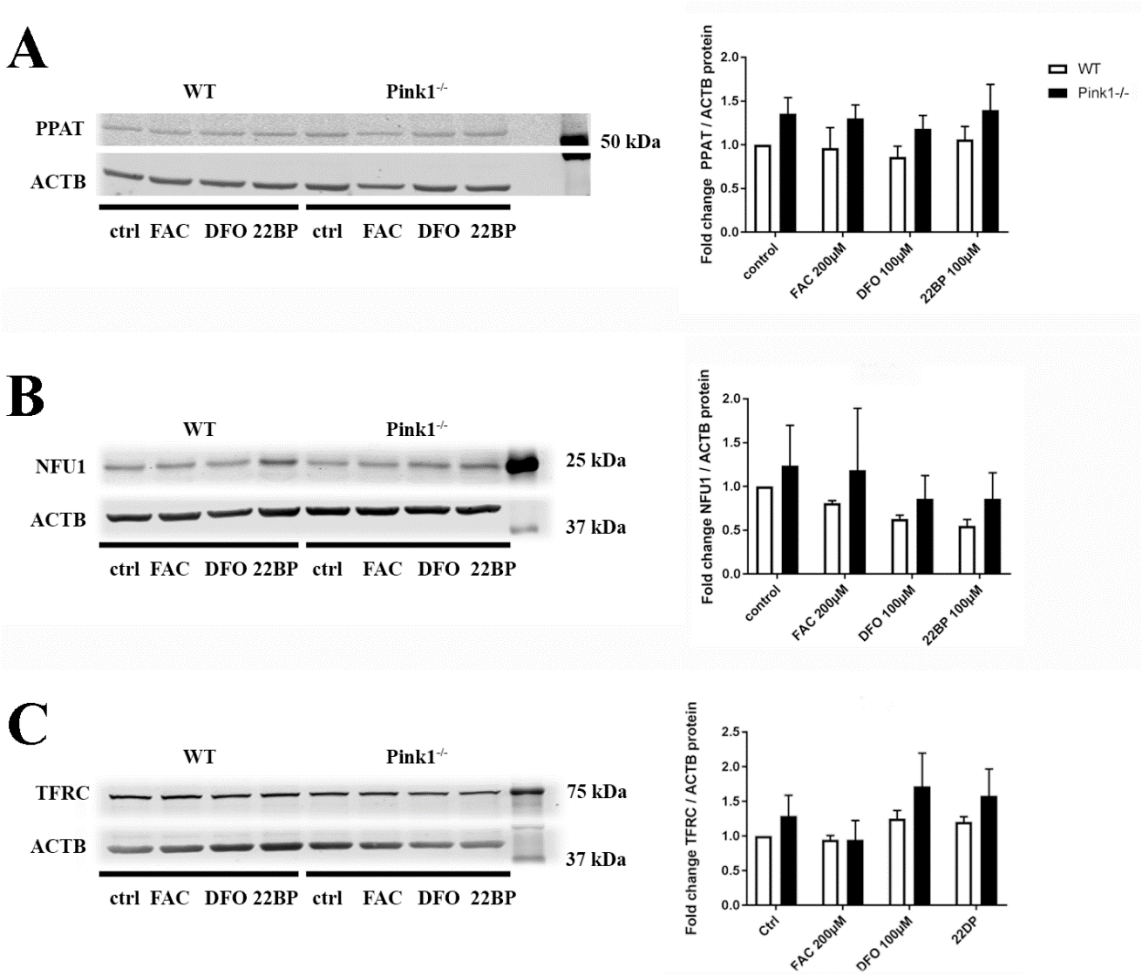

Figure 3. Quantitative immunoblot for **A)** PPAT and **B)** NFU1 and **C)** TFRC in WT and *Pink1*$^{-/-}$ MEF, Ctrl= control condition, after iron overload (FAC) and two different iron depletion conditions (DFO,

Preprints (www.preprints.org) | NOT PEER-REVIEWED | Posted: 22 October 2019 doi:10.20944/preprints201910.0252.v1

22BP). The panels on the right show their densitometric quantifications. n=3, one exemplary set is shown.

It is well known that quantitative immunoblots have difficulties to detect changes that are smaller than two-fold due to the saturation kinetics of membrane and antibody association, whereas the RT-qPCR technique measures its template in linear manner over a wide range of magnitudes. Moreover, the longer half-lives of proteins may require long time-course analyses to demonstrate expression regulations. For most factors in iron homeostasis, ISC and heme turnover, there are no antibodies with sufficient sensitivity and specificity for reliable quantification of the endogenous protein levels. For these reasons, the initial survey of iron effects on homeostasis factors was conducted at the mRNA level. Still, it was disappointing that no significant expression adaptations of PPAT, NFU1 and TRFC protein levels were detectable after 16 h incubation.

2.4 Investigation of Abce1 transcript levels in a larger number of Pink1$^{-/-}$ MEF lines

Again, additional validation experiments were performed to elucidate further what role Pink1 and mitophagy play for iron homeostasis and nucleotide processing. We focused on the ribosomal recycling factor Abce1, which was downregulated to ~0.6-fold after treatment of the cells with iron chelators in 3 WT MEF lines and 3 *Pink1*$^{-/-}$ lines (Figures 1 and 2). *Abce1* was the only factor with a Pink1-dependent expression adaptation (0.70-fold), although not quite significant (p=0.0571). Upon increasing the number of analyzed MEF lines to 7 WT versus 7 *Pink1*$^{-/-}$, the 0.72-fold downregulation of *Abce1* mRNA in *Pink1*$^{-/-}$ cells reached significance (p=0.0240) (Figure 4).

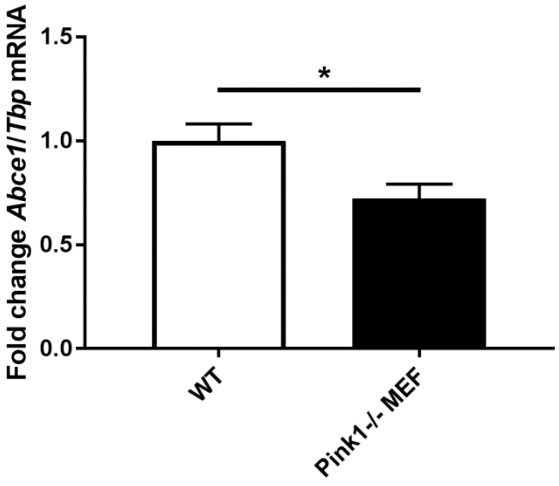

Figure 4. Transcript expression levels of the ISC-containing ribosome recycling factor *Abce1* in WT and *Pink1*$^{-/-}$ MEF (n=7), *: p<0.05

This downregulation of *Abce1* in the absence of *Pink1* was interesting, because this links ribosomal recycling und translation to the availability of iron and nutrients in the cell. These findings not only confirm the previously described connection between mitophagy, iron metabolism and longevity [7], but also extend them to ribosomal translation and ribosome recycling inside mitochondria as well as in the cytosol.

Preprints (www.preprints.org) | NOT PEER-REVIEWED | Posted: 22 October 2019 doi:10.20944/preprints201910.0252.v1

3. Discussion

Our data represent a systematic pioneer effort to document physiological transcriptional regulations of most factors with relevance to iron, ISC and heme homeostasis, after acute changes in iron availability. The immediate expression adaptation after 16 h is best detected at the mRNA level, while protein changes would show much longer delays (see Figure 3). In mammalian fibroblasts, for the first time we explain how iron depletion induces the expression of *Pink1* and *Parkin* as mediators of mitophagy, and how *Pink1*$^{-/-}$ affected mitophagy impairs Abce1-dependent co-translational quality control.

It is important to note that current knowledge believes iron deficiency or hypoxia to act via Hif-1/Fif-2a/Hif-b, triggering a transcriptional induction of *Tfrc* together with *Slc11a2* (Dmt1), *Slc40a1* (Fpn1), *Hmox1*, *Epo* and *Cp* [62]. However, in MEF we observed an opposite regulation of *Tfrc* and *Hmox1* versus *Slc40a1* and *Slc11a2*.

With consistence between WT and mutant cells, iron shortage upregulated the plasma membrane iron import factor *Tfrc* mRNA together with *Ireb2* as stabilizer of its mRNA [77]. Iron depletion also upregulated the mitochondrial membrane iron import factor *Abcb10*. In contrast to this avid activation of iron recruitment proteins upon iron deficiency, the expression of intracellular iron disposal factors was in positive correlation with iron availability. This iron-dependent expression was particularly strong for the endosomal factors Steap2 and Dmt1 (encoded by *Slc11a2*), and exceptionally significant for *Ppat*, *Nthl1*, *Dna2*, *Pold1* and perhaps *Prim2* as components of RNA/DNA surveillance. Figure 5 summarizes our current findings in an overview scheme, indicating transcriptional changes with colored arrows.

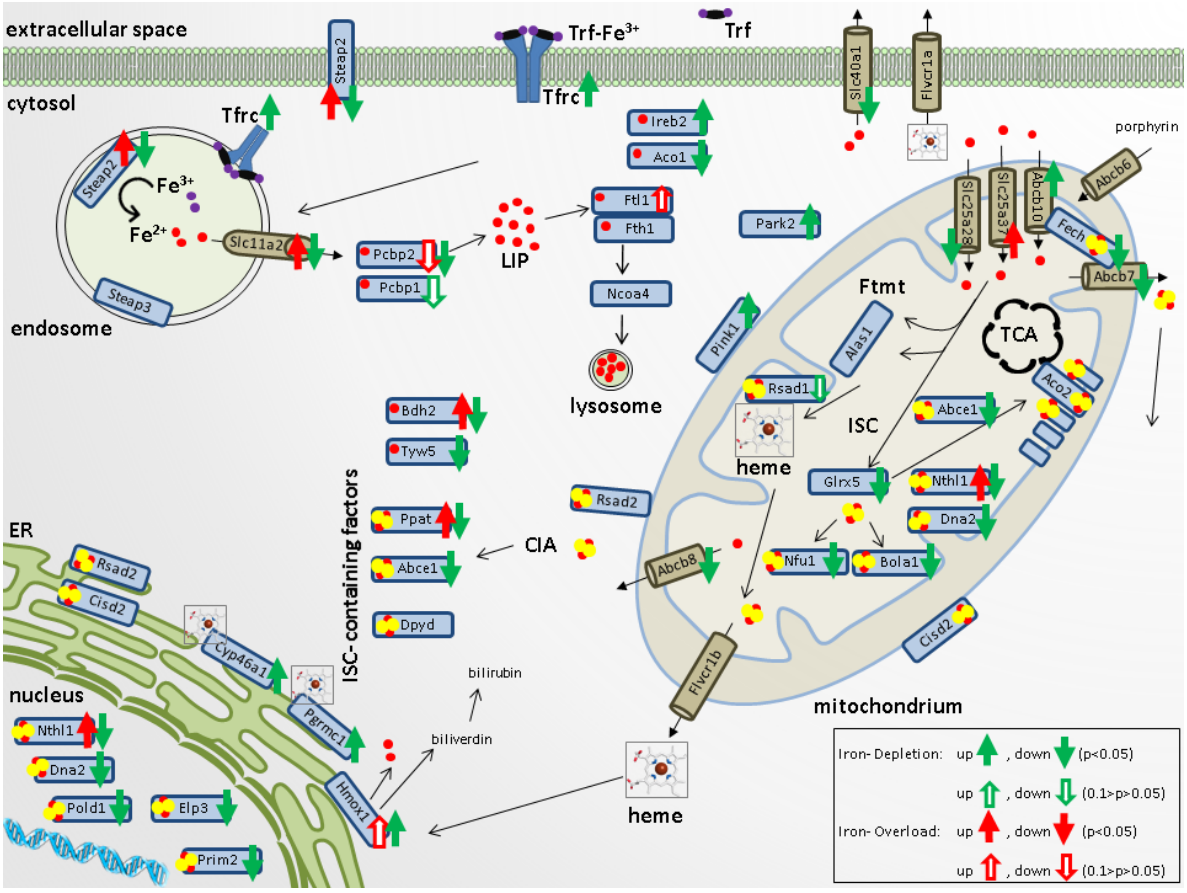

Figure 5. Overview scheme of cellular iron uptake, storage and export, iron transport and processing, mitochondrial iron homeostasis, heme production and turnover, ISC-biogenesis and ISC-binding within the cells. For each factor with significant expression adaptation, green arrows indicate the direction of transcript change during iron depletion, while red arrows refer to iron overload. Ferric iron (Fe^{3+}) is illustrated with purple dots and ferrous iron (Fe^{2+}) with red dots; ISC are represented by red and yellow clusters. CIA: cytosolic iron-

 doi:10.20944/preprints201910.0252.v1

sulfur-cluster assembly machinery, FTMT: mitochondrial ferritin, LIP: labile iron pool; TCA: tricarboxylic acid cycle.

Our novel observation concerning a transcriptional induction of the mitophagy-mediators *Pink1* and *Parkin* in MEF by iron chelators is an important finding to explain the previous reports in *C. elegans* that mitophagy is induced upon iron shortage [7, 8]. A similar induction of *Pink1* and *Parkin* was also reported in human neuroblastoma cells upon deprivation from fetal calf serum, which contains transferrin as the key supplier of iron during cell culture [15]. In the context of human Parkinson pathogenesis, it is noteworthy that the main driver of neurodegeneration in PD, namely the excessive dosage and aggregation of the protein alpha-synuclein, can be modulated by iron via direct binding to an IRE in its mRNA 5'UTR as well as direct binding to the encoded protein [78, 79]. Alpha-synuclein is known to have ferrireductase activity [80-82], with aggregation effects similar to Steap3 [83], and has a physiological localization at the interface between mitochondria and endoplasmic reticulum [84]. It is not possible to investigate the connections between iron and alpha-synuclein further in fibroblasts due to its low expression level in these cells, but it is interesting to note that an 8-fold induction of alpha-synuclein transcripts was observed in human fibroblasts from PD patients with *Pink1* mutation [85]. Thus, both the negative correlation of iron with Pink1/Parkin expression and its positive correlation with alpha-synuclein aggregation may contribute to its toxicity, modulating mitophagy and the neurodegenerative process in PD.

The only expression dysregulation with *Pink1*$^{-/-}$ genotype-dependence was documented for the mRNA of ISC-associated Abce1 under basal conditions without iron manipulation (Figure 2B and Figure 4). These novel mammalian data confirm that Abce1 has a unique link to the mitophagy factor Pink1, as was observed previously also in *D. melanogaster*. These experiments in flies demonstrated that nucleus-derived mRNAs encoding mitochondrial precursor proteins such as the complex-I 30kD subunit continuously translated at the outer mitochondrial membrane surface may be damaged and stall the ribosomal translation machinery during stress periods. This leads to a C-terminal extension of certain amino acids non-coded by mRNA template, which is toxic. In a Pink1-dependent manner, this recruits co-translational quality control factors for RNA/proteins in a process named MISTERMINATE, as well as triggering mitophagy. During this mitochondrial surveillance process, Not4 generates poly-ubiquitin signals on the co-translational control protein Abce1, thus attracting autophagy receptors to the mitochondrial outer membrane and contributing to mitophagy initiation [86, 87]. Thus, fly mitophagy is regulated together with proteostasis in Pink1-dependence via Abce1. It is relevant to note that longevity is increased upon several genetic perturbations of mRNA translation within the mTOR pathway in yeast, *C. elegans* and *D. melanogaster* and by mutations that slow down the expenditure of cellular energy by ribosome biogenesis [88, 89]. Therefore, it will be interesting to assess the lifespan effects of different Abce1 mutations in the future.

Abce1 is one of the most conserved proteins in evolution and is expressed in all organisms except eubacteria. Because of its fundamental role in translation initiation, ribosome biosynthesis and/or ribosome recycling, Abce1 is essential for life. Strong homozygous depletion of the Abce1 homologue pixie in *D. melanogaster* results in early lethality [90]. Also, in mouse, the homozygous knockout of *Abce1* is embryonically lethal, according to the international mouse phenotyping consortium IMPC (https://www.mousephenotype.org/data/genes/MGI:1195458). As an ATPase, Abce1 is responsible for the splitting of the two ribosomal subunits and is thus important for translation termination in mammalian cells, yeast and also archaea. To fulfil these roles, it harbors two essential diamagnetic [4Fe-4S]$^{2+}$ clusters [91]. The depletion of *Abce1* was reported to induce the accumulation of ribosome-associated isolated mRNA-3'-UTRs, consistent with a model of ribosome stalling [92]. It is also known as RNaseL-inhibitor and exerts selective control over the stability of mitochondrial mRNAs during interferon-alpha responses to infection [93]. Decreased ABCE1 protein levels were caused by the induction of ROS and this was attributed to the chelation of iron with subsequent loss of stability of Abce1 [92]. Interestingly, *Abce1* as well as *Hbs1l* transcript levels were shown to be upregulated in the brains of PD patients [87]. Hbs1L is a member of the GTP-binding elongation factor family and was reported to be involved in the regulation of fetal hemoglobin levels [94]. The downregulation of MEF *Abce1* expression in response to iron shortage occurred in parallel to expression downregulation of

 doi:10.20944/preprints201910.0252.v1

several other ISC-associated factors like *Bola1*, *Ppat*, *Nthl1*, *Dna2*, *Prim2* and *Pold1*, probably simply reflecting the limited availability of ISC. Jointly, all these data underline the importance of iron for the RNA/DNA quality surveillance inside and outside mitochondria.

Away from Pink1/Parkin as intrinsic determinants of mitophagy, Parkinson's disease and longevity, the main focus of our study was iron as extrinsic modulator and on the homeostatic expression adaptations induced by it. Important responses to iron depletion included the slight upregulation of *Abcb10* mRNA contrasted by a converse downregulation of *Slc25a28*, although both transporters are thought to mediate iron import. The substrates of Abcb10 transport activity are currently undefined, but its absence was reported to reduce mitoferrin1 protein levels, iron import into mitochondria, heme biosynthesis and hemoglobinization, while a role in the export of ALA was excluded [95]. It is difficult to identify the individual substrates for each mitochondrial transporter protein, given that Abcb10, the putative iron-importer mitoferrin, the heme-synthesis factor ferrochelatase, and the ISC-exporter Abcb7 coexist in a protein complex [61, 62, 66, 96] where the deletion of one member may destabilize its interactors. Similar to Abcb10, a decreased iron import and heme biosynthesis was also shown upon deletion of mitoferrin [97, 98], leading to universal acceptance of mitoferrin as main mitochondrial iron importer [99]. Upon comparison of the transcriptional regulation of both factors, it is intriguing to note that iron shortage leads to parallel induction of *Tfrc* for iron recruitment across plasma membranes, and induction of *Abcb10* which could recruit iron across mitochondrial membranes, but a converse downregulation of *Slc25a28* which encodes mitoferrin-2. Interestingly, the reduction of Slc25a28 in *C. elegans* was reported to result in prolonged lifespan [57]. This paradoxical *Slc25a28* downregulation during iron shortage, however, might be expected for a transporter that mediates iron export, but is unusual for an import factor. In only one study so far, Abcb8 was implicated in mitochondrial export functions for iron and factors required for cytosolic ISC-protein maturation [63]. As expected for mitochondrial iron export factors, *Abcb8* expression was downregulated after iron depletion, to a similar level as *Slc25a28*. Regarding the two mitoferrin isoforms, it was also noteworthy that *Slc25a28* responded to iron depletion, whereas *Slc25a37* seemed regulated only after iron excess. We propose that further studies of transcriptional regulation in response to putative substrate loading would help to elucidate the specific roles of each membrane transporter.

Further mRNA inductions in response to iron deprivation included *Ireb2*/Irp2 as a stabilizer of Tfrc mRNA [77], the over 2-fold induction of the heme-release factor *Pgrmc1* [100], and a massive 4- to 5-fold induction of *Hmox1* (the rate-limiting enzyme in heme-degradation) in response to 22BP, as another possible pathway of iron recruitment. The previously observed impaired *Hmox1* induction after oxidative stress damage in *Pink1*-depleted cells [101] was not detected in MEF in the absence of stress factors. It is interesting to note that iron-starved cells trigger a strong induction of the mitochondrial ferrochelatase-associated heme-release factor *Pgrmc1*, but not a similarly strong effort to export ISC from mitochondria through *Abcb7* induction. The completely novel observation that iron depletion induces *Cyp46a1* as the rate-limiting enzyme of cholesterol degradation provides a hint why iron-deficiency anemia patients show lower blood cholesterol levels, and how iron influences steroidogenesis [102, 103].

Conversely, positive correlation between iron availability and expression levels were observed for numerous intracellular iron-employing factors, particularly *Steap2* and *Dmt1* as components of the endosomal processing, and *Nthl1* and *Ppat*, both of which contain ISC for their proper function. NTHL1 is a DNA N-glycosylase that is localized mainly in the nucleus, but also found in mitochondria [104]. It catalyzes the first step in base excision repair and binds a [4Fe-4S] cluster [55]. *Nthl1* mRNA seemed to react very sensitively with reduction to almost 50% upon iron depletion and induction to 135% after iron overload. This may reflect the known dependence of Nthl1 and Ppat protein stability on the correct ISC insertion [105]. Ppat belongs to the purine/pyrimidine phosphoribosyltransferase family and catalyzes the first step of de novo purine nucleotide biosynthetic pathway. It also possesses a [4Fe-4S] cluster, which is needed for protein maturation [55]. Ppat maturation and subsequent function are affected in the neurodegenerative disorder

 doi:10.20944/preprints201910.0252.v1

Friedreich Ataxia. This disease is caused by loss-of-function mutations in the *Fxn* gene encoding the frataxin protein, which starts the ISC biogenesis within mitochondria [106, 107]. Thus, the transcript reductions of *Nthl1* and *Ppat* probably reflect limited ISC supply from mitochondria.

All other factors with downregulation upon iron deficiency are either involved in the complex synthesis of ISC or contain one or several ISC. Among them were *Bola1*, *Nfu1* and *Glrx5*, which play roles in the synthesis of ISC and are localized inside mitochondria. The cytosolic tRNA modification factor Tyw5 associates with iron and was also drastically reduced after iron deprivation. A slight downregulation was noted for ISC-containing cytosolic Irp1/Aco1 and for ISC-containing Rsad1, which is a heme chaperone in the mitochondrial matrix [108]. In contrast, ISC-containing Rsad2 at the mitochondrial outer membrane and the endoplasmic reticulum [109] was not exhibiting dysregulation in MEF after iron manipulation, despite previous reports on its Pink1-dependence in immune responses [29]. Similarly, ISC-containing Fech in mitochondria was not strongly dysregulated. This indicates that ISC homeostasis is not entirely disrupted upon depletion of extracellular iron or in the absence of *Pink1*, but instead specific vulnerabilities exist, in particular for RNA/DNA quality and genome stability through *Ppat* / *Nthl1* / *Dna2* / *Prim2* / *Pold1* deficiency. This is a central finding, since DNA integrity is crucial for the healthy lifespan [6], and since the DNA repair pathway was recently identified as the most important modifier of onset age and progression velocity in neurodegenerative diseases [110-112].

4. Materials and Methods

Mouse embryonic fibroblast generation:

The mice used were bred at the Central Animal Facility (ZFE) of the Goethe University Medical Faculty in Frankfurt, under FELASA-certified conditions, in accordance with the ETS123 (European Convention for the Protection of Vertebrate Animals), the Council Directive of 24 November 1986 (86/609/EWG) with Annex II and the German Animal Welfare Act. Approval of the local institutional review board (Regierungspraesidium Darmstadt, project V54-19c20/15-FK/1083) was given on 27 March 2017. MEF were prepared from individual embryos at 14.5 days post-coitus of WT and *Pink1*$^{-/-}$ mice, which were generated and bred as previously reported [16]. In brief, embryos were dissected from the uterus, extremities and inner organs were removed and the tissue was treated with 0.05% trypsin (Gibco, Thermo Scientific, Schwerte, Germany) for 10-15 min. Cells were cultivated in Dulbecco's Modified Eagle Medium 4.5 g/l glucose (Invitrogen, Karlsruhe, Germany) plus 15% bovine growth serum (BGS, Thermo Scientific, Schwerte, Germany), 1% glutamine, 1% penicillin and streptomycin (all Invitrogen, Karlsruhe, Germany) at 37 °C and 5% CO2 in a humidified incubator, then *Pink1*$^{-/-}$ cells and their respective littermate WT controls were frozen in liquid nitrogen.

Iron overload / depletion experiments:

MEF cells were plated in 6 well plates (500.000 cells/well) and incubated for 24 h. Cells were either left in normal growth medium or treated with 200 µM ferric ammonium citrate (FAC) (Sigma Aldrich, St. Louis, USA), 100 µM 2,2-bipyridyl (22BP) (Roth, Karlsruhe, Germany), and 100 µM Deferoxamine mesylate (DFO) (Sigma Aldrich, St. Louis, USA) for 16 h and cell pellets were collected for RNA and protein isolation.

Reverse transcriptase real-time quantitative PCR:

For isolation of total RNA, TRI reagent (Sigma Aldrich, St. Louis, USA) was used, and VILO IV (Thermo Scientific, Schwerte, Germany) for reverse transcription, both following manufacturers' instructions. RT-qPCR was performed applying TaqMan Gene Expression Assays (Applied Biosystems, Thermo Scientific, Schwerte, Germany) in cDNA from 20 ng total RNA in 20 µl reactions with 2× master mix (Roche, Basel, Switzerland) in a StepOnePlus Real-Time PCR System (Applied Biosystems, Thermo Scientific, Schwerte, Germany). An RT-qPCR assay of *Pink1* normalized to *Tbp* was used to confirm the genotype in MEFs. For quantification of the individual mRNA levels, the following

 doi:10.20944/preprints201910.0252.v1

TaqMan assays (Thermo Scientific, Schwerte, Germany) were employed: *Abcb6*- Mm00470049_m1, *Abcb7*- Mm01235258_m1, *Abcb8*- Mm00472410_m1, *Abcb10*- Mm00497931_m1, *Abce1*- Mm00649858_m1, *Aco1*- Mm00801417_m1, *Aco2*- Mm00475673_g1, *Alas1*- Mm01235914_m1, *Bach1*- Mm01344527_m1, *Bdh2*- Mm00459075_m1, *Bola1*- Mm01255885_m1, *Brip1*- Mm01297848_m1, *Cdc42bpa*- Mm01322796_m1, *Cisd2*- Mm00835272_m1, *Cp*- Mm00432654_m1, *Cygb* -Mm00446071_m1, *Cyp46a1* -Mm00487306_m1, *Dna2*- Mm01169107_m1, *Dpyd*- Mm00468109_m1, *Elp3*- Mm00804536_m1, *Ercc2*- Mm00514776_m1, *Fdx1*- Mm00433246_m1, *Fech*- Mm00500394_m1, *Flvcr1*- Mm01320423_m1 *Fth1*- Mm00850707_m1, *Ftl1*- Mm03030144_g1, *Ftmt*- Mm01268428_s1, *Fxn*- Mm00784016_s1, *Glrx5*- Mm00511712_m1, *Hebp1*- Mm00469161_m1, *Hmox1*- Mm00516005_m1, *Ireb2*- Mm01179595_m1, *Ncoa4*- Mm00451095_m1, *Nfu1- Mm00777068_m1, Nthl1*- Mm00476559_m1, *Park2*- Mm00450186_m1, *Pcbp1*- Mm00478712_s1, *Pcbp2*- Mm01296174_g1, *Pgrmc1*- Mm00443985_m1, *Pink1*- Mm00550827_m1, *Ppat*- Mm00549096_m1, *Pold1*- Mm00448253_m1, *Prim2*- Mm00477104_m1, *Rsad1*- Mm01296523_m1, *Rsad2*- Mm00491265_m1, *Rtel1*- Mm01220420_m1, *Slc11a2*- Mm00435363_m1, *Slc25a28*- Mm00455077_m1, *Slc25a37*- Mm00471133_m1, *Slc40a1*- Mm01254822_m1, *Steap2*- Mm01320129_m1, *Steap3*- Mm01287243_m1, *Tbp*- Mm00446973_m1, *Tfrc*-Mm00441941_m1, *Trf- Mm00446715_m1, Tyw5*- Mm01254171_m1. Results were analyzed with the $2^{-\Delta\Delta CT}$ method [113].

Quantitative immunoblotting:

Sample preparation for quantitative immunoblotting was done as described before [114]. Samples of 20 μg of protein in 2x Laemmli buffer were heated at 90 °C for 3 min and then separated in 10% tris–glycine polyacrylamide gels, using Precision Plus Protein™ All Blue Standards (Bio-Rad, Hercules, California, USA) as size marker. Transfer to nitrocellulose membranes (Protran, GE Healthcare, Chicago, Illinois, USA) was done at 50 V over 90 min, with blocking in 5% BSA solution in 1x TBS-T for 1 h at room temperature (RT). Primary antibody incubation against PPAT (1:375), NFU1 (1:1000) (both kindly provided by the lab of Prof. Roland Lill) or TFRC (1:500) (Zymed, Thermo Scientific, Schwerte, Germany) occurred overnight at 4 °C. Fluorescence-labeled α-rabbit antibodies (1:15,000 IRDye 680RD, Licor Biosciences, Lincoln, NE, USA) were used as secondary antibodies. Normalization occurred with incubation against beta-Actin (1:2000) (Sigma Aldrich, St. Louis, USA). Fluorescence detection occurred on the Licor Odyssey Classic Instrument and bands were densiometrically analyzed with Image Studio Lite, Version 5.2.

Statistical evaluation:

This was done using Graphpad Prism Version 7 and significant differences were calculated with student's t-test with Welch's correction and one- or two-way ANOVA with subsequent multiple comparison tests.

5. Conclusions

We conducted a pioneer survey of transcriptional responses to extracellular iron changes, using murine fibroblasts. Iron deprivation triggers not only the known induction of *Tfrc* mRNA and its stabilization by additional Irp2 synthesis, but also strong expression of *Pgrmc1* and *Hmox1* for cytosolic heme breakdown and a novel induction of the mitochondrial membrane transporter *Abcb10* mRNA. The mitoferrin-1 encoding mRNA *Slc25a37* showed induction after iron excess, while the mitoferrin-2 encoding mRNA *Slc25a28* was decreased similar to the export factors *Abcb7* and *Abcb8* after iron deprivation. These findings shed new light on the question how the two mitoferrins, Abcb10, Abcb7 and Abcb8 complement each other in the regulation of iron import and export in mitochondria. Iron shortage also triggers several-fold transcript induction for the mitophagy regulators *Pink1* and *Parkin* within 16 h. Conversely, iron availability correlates positively with expression of *Steap2* and *Dmt1* as iron-processing factors in the endosome, and expression of ISC-containing factor *Nthl1* for DNA quality control / integrity in nucleus / mitochondria as well as of ISC-containing factor *Ppat* for nucleotide production in cytosol. Also the ISC-containing factors *Dna2*,

 doi:10.20944/preprints201910.0252.v1

Prim2, and Pold1 showed downregulated expression during iron depletion, suggesting impaired DNA quality surveillance. In comparison to the strong impact of iron chelation on the initiation of mitophagy, only one mild reverse feedback effect from mitophagy onto iron usage was noted, namely the Pink1-ablation mediated deficit in *Abce1* transcript levels. This is the first evidence in mammals for the existence of a Pink1-dependent mechanism described previously in *D. melanogaster*, where nucleus-encoded mRNAs and the corresponding precursor proteins for mitochondria undergo a co-translational quality control by Abce1, in parallel to the mitophagic elimination of dysfunctional mitochondrial fragments. Overall, our work identifies specific factors of iron homeostasis and iron-dependent cellular processes, which respond in sensitive and selective manner to iron manipulation. Particularly the impairment of DNA repair is known as a modifier of lifespan and a risk factor of neurodegenerative diseases. In view of iron accumulation in the brain of PD patients and known iron toxicity, these findings may have therapeutic applications. Overall, the factors identified act via iron homeostasis and mitophagy and contribute to the modification of the healthy lifespan.

Supplementary Materials: The following are available online. Supplementary Figure S1: mRNA expression analysis by RT-qPCR in WT and *Pink1*$^{-/-}$ MEF (n=3versus3) regarding factors related to iron homeostasis or utilization. All factors are presented in alphabetical order. Their expression adaptation was documented after iron overload (FAC) and under two different iron depletion conditions (DFO, 22BP). Mean values with SEM are shown, normalized to the control condition. The levels of significance are illustrated by symbols T: 0.1>p>0.05, *: p< 0.05, **: p < 0.01, ***: p < 0.001, ****: p < 0.0001. Asterisks represent significance in wildtype MEF in respect to WT control and hashtags in *Pink1*$^{-/-}$ MEF, in respect to knockout control.

Author Contributions: Conceptualization, G.A.; methodology, G.A., J.K., N.E.S., A.A., S.K., R.H., S.G.; writing—original draft preparation, G.A., J.K.; writing—review and editing, all authors; funding acquisition, G.A.

Funding: This research was funded by the German Federal Ministry of Education through the National Genome Research Network (NGFNplus, Bundesministerium für Bildung und Forschung, 01GS08138), the GerontoMitoSys network (Bundesministerium für Bildung und Forschung, PTJ 0315584A) and by the European Union (ERAnet-RePARK, DLR 01EW1012).

Acknowledgments: The authors thank Prof. Roland Lill and Dr. Oliver Stehling for helpful discussions and providing antibodies. We thank Gabriele Köpf for excellent technical support.

Conflicts of Interest: The authors declare no conflict of interest.

Abbreviations

µM	MicroMolar
22BP	2,2′-Bipyridine
AAA+	ATPases associated with diverse cellular activities
Abcb10	ATP binding cassette subfamily B member 10
Abcb7	ATP binding cassette subfamily B member 7
Abcb8	ATP binding cassette subfamily B member 8
Abce1	ATP binding cassette subfamily E member 1, RNase L inhibitor 1
Aco1	Aconitase 1, cytoplasmic, aka Irp1, aka Ferritin repressor protein
Aco2	Aconitase 2, mitochondrial
ACTB	Actin beta
Alas1	5'-aminolevulinate synthase 1
ANOVA	Analysis of variance
ATPase	Adenosintriphosphatase
Bdh2	3-hydroxybutyrate dehydrogenase-2
Bola1	BolA Family Member 1
Brip1	Brca1 Interacting Protein C-Terminal Helicase 1, Fancj
Cdc42bpa	Cdc42 binding protein kinase alpha (Dmpk-like), Mrcka
CIA	Cytosolic iron- sulfur cluster assembly machinery
Cisd2	CDGSH iron- sulfur domain 2, Wfs2
CO_2	Carbon dioxide

 doi:10.20944/preprints201910.0252.v1

Cp	Ceruploplasmin
DFO	Deferoxamine
Cyp46a1	Cytochrome P450 Family 46 Subfamily A Member 1
Dmt1	Divalent metal transporter 1, encoded by *Slc11a2*
DNA	Desoxyribonucleic acid
Dna2	DNA replication helicase/nuclease 2
Dpyd	Dihydropyrimidine dehydrogenase
Elp3	Elongator acetyltransferase complex subunit 3
ER	Endoplasmic reticulum
Ercc2	ERCC excision repair 2, TFIIH core complex helicase subunit, Cxpd
FAC	Ferric ammonium acid
Fdx1	Ferredoxin 1, mitochondrial Adrenodoxin
Fech	Ferrochelatase, Heme synthase
Flvcr1a	Feline leukemia virus subgroup C cellular receptor 1a, Pcarp
Flvcr1b	Feline leukemia virus subgroup C cellular receptor 1b, Pcarp
Fth1	Ferritin heavy chain
Ftl1	Ferritin light chain
Ftmt	Mitochondrial ferritin
Fxn	Frataxin, Frda
g	Gram
Glrx5	Glutaredoxin 5
h	Hour
Hbs1l	Hbs1 like translational GTPase, Erfs
Hebp1	Heme binding protein 1
Hmox1	Heme oxygenase 1, HO-1
IMPC	International mouse phenotyping consortium
IRE	Iron response element
Ireb1	Iron-responsive element-binding protein 1 (=Irp1), encoded by *Aco1*
Ireb2	Iron-responsive element-binding protein 2 (=Irp2), encoded by *Ireb2*
Irp1	Iron regulatory protein 1 (=cytosolic aconitase=Ireb1), encoded by *Aco1*
Irp2	Iron regulatory protein 2 (=Aco3=Ireb2), encoded by *Ireb2* mRNA
ISC	Iron sulfur cluster
l	Liter
LIP	Labile iron pool
MEF	Mouse embryonic fibroblast
Mfrn1	Mitoferrin 1, encoded by *Slc25a37*
Mfrn2	Mitoferrin 2, encoded by *Slc25a28*
min	Minute
mRNA	Messenger ribonucleic acid
mTOR	Mechanistic target of rapamycin kinase
MPTP	1-methyl-4-phenyl-1,2,3,6-tetrahydropyridine
Ncoa4	Nuclear receptor coactivator 4
Nfu1	Nfu1 iron-sulfur cluster scaffold
Not4	Ccr4-Not transcription complex subunit 4
Nthl1	Nth like DNA glycosylase 1
Parkin	Parkinson disease protein 2
Pcbp1	Poly(RC) binding protein 1, hnRNP-E1
Pcbp2	Poly(RC) binding protein 2, hnRNP-E2
PD	Parkinson's disease
Pgrmc1	Progesterone receptor membrane component 1, Dap1
Pink1	PTEN induced kinase 1
Pold1	DNA polymerase delta 1 catalytic subunit, Cdc2 homolog
Ppat	Phosphoribosyl pyrophosphate amidotransferase, Gpat, ATase

 doi:10.20944/preprints201910.0252.v1

Prim2	DNA primase subunit 2
RNA	Ribonucleic acid
ROS	Reactive oxygen species
Rsad1	Radical S-adenosyl methionine domain containing 1
Rsad2	Radical S-adenosyl methionine domain containing 2, Viperin
RT	Room temperature
Rtel1	Regulator of telomere elongation helicase 1
SEM	Standard error of the mean
Slc11a2	Solute carrier family 11 member 2, Divalent metal transporter 1, Dmt1
Slc25a37	Solute carrier family 25 member 37, Mitoferrin 1
Slc25a28	Solute carrier family 25 member 28, Mitoferrin 2
Slc40a1	Solute carrier family 40 member 1, Ferroportin 1, Ireg1
Steap2	Six transmembrane epithelial antigen of the prostate 2, Stmp
Steap3	Six transmembrane epithelial antigen of the prostate 3, Stmp3
Tbp	Tata-binding protein
TBST	Tris-buffered saline/Tween 20
TCA	Tricarboxylic acid cycle
Trf	Transferrin
Tfrc	Transferrin receptor 1
Tyw5	tRNA Wybutosine synthesizing protein 5
UTR	Untranslated region
V	Volt
WT	Wildtype

References

1. Huang, C.Y., et al., *A review on the effects of current chemotherapy drugs and natural agents in treating non-small cell lung cancer.* Biomedicine (Taipei), 2017. **7**(4): p. 23.
2. Becker, L.A., et al., *Therapeutic reduction of ataxin-2 extends lifespan and reduces pathology in TDP-43 mice.* Nature, 2017. **544**(7650): p. 367-371.
3. Bishop, N.A. and L. Guarente, *Genetic links between diet and lifespan: shared mechanisms from yeast to humans.* Nature reviews. Genetics, 2007. **8**(11): p. 835-44.
4. Vijg, J. and J. Campisi, *Puzzles, promises and a cure for ageing.* Nature, 2008. **454**(7208): p. 1065-71.
5. Finkel, T., *The metabolic regulation of aging.* Nature medicine, 2015. **21**(12): p. 1416-23.
6. Latorre-Pellicer, A., et al., *Mitochondrial and nuclear DNA matching shapes metabolism and healthy ageing.* Nature, 2016. **535**(7613): p. 561-5.
7. Schiavi, A., et al., *Iron-Starvation-Induced Mitophagy Mediates Lifespan Extension upon Mitochondrial Stress in C. elegans.* Current biology : CB, 2015. **25**(14): p. 1810-22.
8. Ryu, D., et al., *Urolithin A induces mitophagy and prolongs lifespan in C. elegans and increases muscle function in rodents.* Nat Med, 2016. **22**(8): p. 879-88.
9. Corti, O., S. Lesage, and A. Brice, *What genetics tells us about the causes and mechanisms of Parkinson's disease.* Physiological reviews, 2011. **91**(4): p. 1161-218.
10. Valente, E.M., et al., *Hereditary early-onset Parkinson's disease caused by mutations in PINK1.* Science, 2004. **304**(5674): p. 1158-60.

11. Exner, N., et al., *Loss-of-function of human PINK1 results in mitochondrial pathology and can be rescued by parkin.* The Journal of neuroscience : the official journal of the Society for Neuroscience, 2007. **27**(45): p. 12413-8.
12. Matsuda, N. and K. Tanaka, *Uncovering the roles of PINK1 and parkin in mitophagy.* Autophagy, 2010. **6**(7): p. 952-4.
13. Hoepken, H.H., et al., *Mitochondrial dysfunction, peroxidation damage and changes in glutathione metabolism in PARK6.* Neurobiology of disease, 2007. **25**(2): p. 401-11.
14. Parganlija, D., et al., *Loss of PINK1 impairs stress-induced autophagy and cell survival.* PloS one, 2014. **9**(4): p. e95288.
15. Klinkenberg, M., et al., *Restriction of trophic factors and nutrients induces PARKIN expression.* Neurogenetics, 2012. **13**(1): p. 9-21.
16. Gispert, S., et al., *Parkinson phenotype in aged PINK1-deficient mice is accompanied by progressive mitochondrial dysfunction in absence of neurodegeneration.* PloS one, 2009. **4**(6): p. e5777.
17. Visanji, N.P., et al., *Iron deficiency in parkinsonism: region-specific iron dysregulation in Parkinson's disease and multiple system atrophy.* J Parkinsons Dis, 2013. **3**(4): p. 523-37.
18. Ndayisaba, A., C. Kaindlstorfer, and G.K. Wenning, *Iron in Neurodegeneration - Cause or Consequence?* Front Neurosci, 2019. **13**: p. 180.
19. Wang, J.Y., et al., *Meta-analysis of brain iron levels of Parkinson's disease patients determined by postmortem and MRI measurements.* Sci Rep, 2016. **6**: p. 36669.
20. Lei, P., et al., *Tau deficiency induces parkinsonism with dementia by impairing APP-mediated iron export.* Nat Med, 2012. **18**(2): p. 291-5.
21. You, L.H., et al., *Mitochondrial ferritin suppresses MPTP-induced cell damage by regulating iron metabolism and attenuating oxidative stress.* Brain Res, 2016. **1642**: p. 33-42.
22. Schweitzer, K.J., et al., *Transcranial ultrasound in different monogenetic subtypes of Parkinson's disease.* Journal of neurology, 2007. **254**(5): p. 613-6.
23. Li, C., et al., *PINK1 and PARK2 Suppress Pancreatic Tumorigenesis through Control of Mitochondrial Iron-Mediated Immunometabolism.* Dev Cell, 2018. **46**(4): p. 441-455 e8.
24. Kang, R., et al., *Mitochondrial quality control mediated by PINK1 and PRKN: links to iron metabolism and tumor immunity.* Autophagy, 2019. **15**(1): p. 172-173.
25. Allen, G.F., et al., *Loss of iron triggers PINK1/Parkin-independent mitophagy.* EMBO reports, 2013. **14**(12): p. 1127-35.
26. Esposito, G., et al., *Aconitase causes iron toxicity in Drosophila pink1 mutants.* PLoS genetics, 2013. **9**(4): p. e1003478.
27. Auburger, G., S. Gispert, and N. Brehm, *Methyl-Arginine Profile of Brain from Aged PINK1-KO+A53T-SNCA Mice Suggests Altered Mitochondrial Biogenesis.* Parkinson's disease, 2016. **2016**: p. 4686185.
28. Auburger, G., et al., *SerThr-PhosphoProteome of Brain from Aged PINK1-KO+A53T-SNCA Mice Reveals pT1928-MAP1B and pS3781-ANK2 Deficits, as Hub between Autophagy and Synapse Changes.* International journal of molecular sciences, 2019. **20**(13).
29. Torres-Odio, S., et al., *Progression of pathology in PINK1-deficient mouse brain from splicing via ubiquitination, ER stress, and mitophagy changes to neuroinflammation.* J Neuroinflammation, 2017. **14**(1): p. 154.
30. Gispert, S., et al., *Potentiation of neurotoxicity in double-mutant mice with Pink1 ablation and A53T-SNCA overexpression.* Human molecular genetics, 2015. **24**(4): p. 1061-76.

31. Pickrell, A.M., et al., *Endogenous Parkin Preserves Dopaminergic Substantia Nigral Neurons following Mitochondrial DNA Mutagenic Stress.* Neuron, 2015. **87**(2): p. 371-81.
32. Sliter, D.A., et al., *Parkin and PINK1 mitigate STING-induced inflammation.* Nature, 2018. **561**(7722): p. 258-262.
33. Matheoud, D., et al., *Intestinal infection triggers Parkinson's disease-like symptoms in Pink1(-/-) mice.* Nature, 2019.
34. Manzanillo, P.S., et al., *The ubiquitin ligase parkin mediates resistance to intracellular pathogens.* Nature, 2013. **501**(7468): p. 512-6.
35. Clark, I.E., et al., *Drosophila pink1 is required for mitochondrial function and interacts genetically with parkin.* Nature, 2006. **441**(7097): p. 1162-6.
36. Saini, N., et al., *Extended lifespan of Drosophila parkin mutants through sequestration of redox-active metals and enhancement of anti-oxidative pathways.* Neurobiol Dis, 2010. **40**(1): p. 82-92.
37. Cooper, J.F., et al., *Activation of the mitochondrial unfolded protein response promotes longevity and dopamine neuron survival in Parkinson's disease models.* Sci Rep, 2017. **7**(1): p. 16441.
38. Nakamura, S. and T. Yoshimori, *Autophagy and Longevity.* Mol Cells, 2018. **41**(1): p. 65-72.
39. Munkacsy, E. and S.L. Rea, *The paradox of mitochondrial dysfunction and extended longevity.* Exp Gerontol, 2014. **56**: p. 221-33.
40. Butler, J.A., et al., *Long-lived mitochondrial (Mit) mutants of Caenorhabditis elegans utilize a novel metabolism.* FASEB J, 2010. **24**(12): p. 4977-88.
41. Fischer, F., et al., *Human CLPP reverts the longevity phenotype of a fungal ClpP deletion strain.* Nat Commun, 2013. **4**: p. 1397.
42. Gispert, S., et al., *Loss of mitochondrial peptidase Clpp leads to infertility, hearing loss plus growth retardation via accumulation of CLPX, mtDNA and inflammatory factors.* Human molecular genetics, 2013. **22**(24): p. 4871-87.
43. Bhaskaran, S., et al., *Loss of mitochondrial protease ClpP protects mice from diet-induced obesity and insulin resistance.* EMBO reports, 2018. **19**(3).
44. Mai, S., et al., *Decreased expression of Drp1 and Fis1 mediates mitochondrial elongation in senescent cells and enhances resistance to oxidative stress through PINK1.* Journal of cell science, 2010. **123**(Pt 6): p. 917-26.
45. Seo, J.H., et al., *The Mitochondrial Unfoldase-Peptidase Complex ClpXP Controls Bioenergetics Stress and Metastasis.* PLoS biology, 2016. **14**(7): p. e1002507.
46. Alexeyev, M.F., *Is there more to aging than mitochondrial DNA and reactive oxygen species?* FEBS J, 2009. **276**(20): p. 5768-87.
47. Hwang, A.B., D.E. Jeong, and S.J. Lee, *Mitochondria and organismal longevity.* Curr Genomics, 2012. **13**(7): p. 519-32.
48. Stehling, O. and R. Lill, *The role of mitochondria in cellular iron-sulfur protein biogenesis: mechanisms, connected processes, and diseases.* Cold Spring Harbor perspectives in biology, 2013. **5**(8): p. a011312.
49. Stehling, O., C. Wilbrecht, and R. Lill, *Mitochondrial iron-sulfur protein biogenesis and human disease.* Biochimie, 2014. **100**: p. 61-77.
50. Kafina, M.D. and B.H. Paw, *Intracellular iron and heme trafficking and metabolism in developing erythroblasts.* Metallomics : integrated biometal science, 2017. **9**(9): p. 1193-1203.
51. Barupala, D.P., et al., *Synthesis, delivery and regulation of eukaryotic heme and Fe-S cluster cofactors.* Archives of biochemistry and biophysics, 2016. **592**: p. 60-75.

52. Kimura, S. and T. Suzuki, *Iron-sulfur proteins responsible for RNA modifications.* Biochimica et biophysica acta, 2015. **1853**(6): p. 1272-83.
53. Lill, R., *Function and biogenesis of iron-sulphur proteins.* Nature, 2009. **460**(7257): p. 831-8.
54. Puig, S., et al., *The elemental role of iron in DNA synthesis and repair.* Metallomics : integrated biometal science, 2017. **9**(11): p. 1483-1500.
55. Paul, V.D. and R. Lill, *Biogenesis of cytosolic and nuclear iron-sulfur proteins and their role in genome stability.* Biochimica et biophysica acta, 2015. **1853**(6): p. 1528-39.
56. Furuyama, K., K. Kaneko, and P.D. Vargas, *Heme as a magnificent molecule with multiple missions: heme determines its own fate and governs cellular homeostasis.* The Tohoku journal of experimental medicine, 2007. **213**(1): p. 1-16.
57. Ren, Y., et al., *Reduction of mitoferrin results in abnormal development and extended lifespan in Caenorhabditis elegans.* PloS one, 2012. **7**(1): p. e29666.
58. Yanatori, I., et al., *The iron chaperone poly(rC)-binding protein 2 forms a metabolon with the heme oxygenase 1/cytochrome P450 reductase complex for heme catabolism and iron transfer.* J Biol Chem, 2017. **292**(32): p. 13205-13229.
59. Galy, B., et al., *Iron regulatory proteins secure mitochondrial iron sufficiency and function.* Cell metabolism, 2010. **12**(2): p. 194-201.
60. Li, H., et al., *Iron regulatory protein deficiency compromises mitochondrial function in murine embryonic fibroblasts.* Sci Rep, 2018. **8**(1): p. 5118.
61. Chen, W., H.A. Dailey, and B.H. Paw, *Ferrochelatase forms an oligomeric complex with mitoferrin-1 and Abcb10 for erythroid heme biosynthesis.* Blood, 2010. **116**(4): p. 628-30.
62. Lane, D.J., et al., *Cellular iron uptake, trafficking and metabolism: Key molecules and mechanisms and their roles in disease.* Biochimica et biophysica acta, 2015. **1853**(5): p. 1130-44.
63. Ichikawa, Y., et al., *Disruption of ATP-binding cassette B8 in mice leads to cardiomyopathy through a decrease in mitochondrial iron export.* Proceedings of the National Academy of Sciences of the United States of America, 2012. **109**(11): p. 4152-7.
64. Pondarre, C., et al., *The mitochondrial ATP-binding cassette transporter Abcb7 is essential in mice and participates in cytosolic iron-sulfur cluster biogenesis.* Human molecular genetics, 2006. **15**(6): p. 953-64.
65. Lill, R., et al., *The role of mitochondria and the CIA machinery in the maturation of cytosolic and nuclear iron-sulfur proteins.* Eur J Cell Biol, 2015. **94**(7-9): p. 280-91.
66. Maio, N., et al., *Dimeric ferrochelatase bridges ABCB7 and ABCB10 homodimers in an architecturally defined molecular complex required for heme biosynthesis.* Haematologica, 2019.
67. Maio, N. and T.A. Rouault, *Mammalian Fe-S proteins: definition of a consensus motif recognized by the co-chaperone HSC20.* Metallomics : integrated biometal science, 2016. **8**(10): p. 1032-1046.
68. Uzarska, M.A., et al., *Mitochondrial Bol1 and Bol3 function as assembly factors for specific iron-sulfur proteins.* eLife, 2016. **5**.
69. Braymer, J.J. and R. Lill, *Iron-sulfur cluster biogenesis and trafficking in mitochondria.* J Biol Chem, 2017. **292**(31): p. 12754-12763.
70. Choi, A.M. and J. Alam, *Heme oxygenase-1: function, regulation, and implication of a novel stress-inducible protein in oxidant-induced lung injury.* Am J Respir Cell Mol Biol, 1996. **15**(1): p. 9-19.
71. Mast, N., et al., *Structural basis of drug binding to CYP46A1, an enzyme that controls cholesterol turnover in the brain.* J Biol Chem, 2010. **285**(41): p. 31783-95.

72. Correia, M.A., P.R. Sinclair, and F. De Matteis, *Cytochrome P450 regulation: the interplay between its heme and apoprotein moieties in synthesis, assembly, repair, and disposal.* Drug Metab Rev, 2011. **43**(1): p. 1-26.
73. de Sanctis, D., et al., *Crystal structure of cytoglobin: the fourth globin type discovered in man displays heme hexa-coordination.* J Mol Biol, 2004. **336**(4): p. 917-27.
74. Barthelme, D., et al., *Structural organization of essential iron-sulfur clusters in the evolutionarily highly conserved ATP-binding cassette protein ABCE1.* J Biol Chem, 2007. **282**(19): p. 14598-607.
75. Alhebshi, A., et al., *The essential iron-sulfur protein Rli1 is an important target accounting for inhibition of cell growth by reactive oxygen species.* Mol Biol Cell, 2012. **23**(18): p. 3582-90.
76. Huang, B., M.J. Johansson, and A.S. Bystrom, *An early step in wobble uridine tRNA modification requires the Elongator complex.* RNA, 2005. **11**(4): p. 424-36.
77. Erlitzki, R., J.C. Long, and E.C. Theil, *Multiple, conserved iron-responsive elements in the 3'-untranslated region of transferrin receptor mRNA enhance binding of iron regulatory protein 2.* The Journal of biological chemistry, 2002. **277**(45): p. 42579-87.
78. Wolozin, B. and N. Golts, *Iron and Parkinson's disease.* Neuroscientist, 2002. **8**(1): p. 22-32.
79. Chen, B., et al., *Interactions between iron and alpha-synuclein pathology in Parkinson's disease.* Free radical biology & medicine, 2019. **141**: p. 253-260.
80. Brown, D.R., *alpha-Synuclein as a ferrireductase.* Biochemical Society transactions, 2013. **41**(6): p. 1513-7.
81. McDowall, J.S., et al., *Alpha-synuclein ferrireductase activity is detectible in vivo, is altered in Parkinson's disease and increases the neurotoxicity of DOPAL.* Molecular and cellular neurosciences, 2017. **85**: p. 1-11.
82. McDowall, J.S. and D.R. Brown, *Alpha-synuclein: relating metals to structure, function and inhibition.* Metallomics : integrated biometal science, 2016. **8**(4): p. 385-97.
83. Roberts, H.L., B.L. Schneider, and D.R. Brown, *alpha-Synuclein increases beta-amyloid secretion by promoting beta-/gamma-secretase processing of APP.* PloS one, 2017. **12**(2): p. e0171925.
84. Guardia-Laguarta, C., et al., *A new role for alpha-synuclein in Parkinson's disease: Alteration of ER-mitochondrial communication.* Movement disorders : official journal of the Movement Disorder Society, 2015. **30**(8): p. 1026-33.
85. Hoepken, H.H., et al., *Parkinson patient fibroblasts show increased alpha-synuclein expression.* Experimental neurology, 2008. **212**(2): p. 307-13.
86. Wu, Z., et al., *MISTERMINATE Mechanistically Links Mitochondrial Dysfunction with Proteostasis Failure.* Mol Cell, 2019.
87. Wu, Z., et al., *Ubiquitination of ABCE1 by NOT4 in Response to Mitochondrial Damage Links Co-translational Quality Control to PINK1-Directed Mitophagy.* Cell metabolism, 2018. **28**(1): p. 130-144 e7.
88. Mehta, R., et al., *Regulation of mRNA translation as a conserved mechanism of longevity control.* Adv Exp Med Biol, 2010. **694**: p. 14-29.
89. MacInnes, A.W., *The role of the ribosome in the regulation of longevity and lifespan extension.* Wiley Interdiscip Rev RNA, 2016. **7**(2): p. 198-212.
90. Coelho, C.M., et al., *Growth and cell survival are unevenly impaired in pixie mutant wing discs.* Development, 2005. **132**(24): p. 5411-24.
91. Nurenberg-Goloub, E., et al., *Ribosome recycling is coordinated by processive events in two asymmetric ATP sites of ABCE1.* Life Sci Alliance, 2018. **1**(3).
92. Sudmant, P.H., et al., *Widespread Accumulation of Ribosome-Associated Isolated 3' UTRs in Neuronal Cell Populations of the Aging Brain.* Cell Rep, 2018. **25**(9): p. 2447-2456 e4.

93. Le Roy, F., et al., *The 2-5A/RNase L/RNase L inhibitor (RLI) [correction of (RNI)] pathway regulates mitochondrial mRNAs stability in interferon alpha-treated H9 cells.* The Journal of biological chemistry, 2001. **276**(51): p. 48473-82.
94. Stadhouders, R., et al., *HBS1L-MYB intergenic variants modulate fetal hemoglobin via long-range MYB enhancers.* J Clin Invest, 2014. **124**(4): p. 1699-710.
95. Seguin, A., et al., *Reductions in the mitochondrial ABC transporter Abcb10 affect the transcriptional profile of heme biosynthesis genes.* J Biol Chem, 2017. **292**(39): p. 16284-16299.
96. Chen, W., et al., *Abcb10 physically interacts with mitoferrin-1 (Slc25a37) to enhance its stability and function in the erythroid mitochondria.* Proceedings of the National Academy of Sciences of the United States of America, 2009. **106**(38): p. 16263-8.
97. Shaw, G.C., et al., *Mitoferrin is essential for erythroid iron assimilation.* Nature, 2006. **440**(7080): p. 96-100.
98. Paradkar, P.N., et al., *Regulation of mitochondrial iron import through differential turnover of mitoferrin 1 and mitoferrin 2.* Mol Cell Biol, 2009. **29**(4): p. 1007-16.
99. Muhlenhoff, U., et al., *Compartmentalization of iron between mitochondria and the cytosol and its regulation.* European journal of cell biology, 2015. **94**(7-9): p. 292-308.
100. Piel, R.B., 3rd, et al., *A Novel Role for Progesterone Receptor Membrane Component 1 (PGRMC1): A Partner and Regulator of Ferrochelatase.* Biochemistry, 2016. **55**(37): p. 5204-17.
101. Sheng, X.J., et al., *Antagonism of proteasome inhibitor-induced heme oxygenase-1 expression by PINK1 mutation.* PloS one, 2017. **12**(8): p. e0183076.
102. Choi, J.W., S.K. Kim, and S.H. Pai, *Changes in serum lipid concentrations during iron depletion and after iron supplementation.* Annals of clinical and laboratory science, 2001. **31**(2): p. 151-6.
103. Llorens, J.V., et al., *Mitochondrial iron supply is required for the developmental pulse of ecdysone biosynthesis that initiates metamorphosis in Drosophila melanogaster.* Journal of biological inorganic chemistry : JBIC : a publication of the Society of Biological Inorganic Chemistry, 2015. **20**(8): p. 1229-38.
104. Li, J., A. Braganza, and R.W. Sobol, *Base excision repair facilitates a functional relationship between Guanine oxidation and histone demethylation.* Antioxid Redox Signal, 2013. **18**(18): p. 2429-43.
105. Crooks, D.R., et al., *Acute loss of iron-sulfur clusters results in metabolic reprogramming and generation of lipid droplets in mammalian cells.* J Biol Chem, 2018. **293**(21): p. 8297-8311.
106. Martelli, A., et al., *Frataxin is essential for extramitochondrial Fe-S cluster proteins in mammalian tissues.* Human molecular genetics, 2007. **16**(22): p. 2651-8.
107. Vaubel, R.A. and G. Isaya, *Iron-sulfur cluster synthesis, iron homeostasis and oxidative stress in Friedreich ataxia.* Mol Cell Neurosci, 2013. **55**: p. 50-61.
108. Haskamp, V., et al., *The radical SAM protein HemW is a heme chaperone.* J Biol Chem, 2018. **293**(7): p. 2558-2572.
109. Hinson, E.R. and P. Cresswell, *The N-terminal amphipathic alpha-helix of viperin mediates localization to the cytosolic face of the endoplasmic reticulum and inhibits protein secretion.* J Biol Chem, 2009. **284**(7): p. 4705-12.
110. Consortium., G.M.o.H.s.D.G.-H., *Identification of Genetic Factors that Modify Clinical Onset of Huntington's Disease.* Cell, 2015. **162**(3): p. 516-26.
111. Jones, L., H. Houlden, and S.J. Tabrizi, *DNA repair in the trinucleotide repeat disorders.* The Lancet. Neurology, 2017. **16**(1): p. 88-96.
112. McKinnon, P.J. and K.W. Caldecott, *DNA strand break repair and human genetic disease.* Annual review of genomics and human genetics, 2007. **8**: p. 37-55.

 doi:10.20944/preprints201910.0252.v1

113. Schmittgen, T.D. and K.J. Livak, *Analyzing real-time PCR data by the comparative C(T) method.* Nat Protoc, 2008. **3**(6): p. 1101-8.

114. Sen, N.E., et al., *Generation of an Atxn2-CAG100 knock-in mouse reveals N-acetylaspartate production deficit due to early Nat8l dysregulation.* Neurobiology of disease, 2019. **132**: p. 104559.